The Meteoritical Society

*Meteoritics & Planetary Science* 49, Nr 4, 576–594 (2014)
doi: 10.1111/maps.12275

# He and Ne in individual chromite grains from the regolith breccia Ghubara (L5): Exploring the history of the L chondrite parent body regolith

Matthias M. M. MEIER[1,2*], Birger SCHMITZ[2], Carl ALWMARK[1], Reto TRAPPITSCH[3], Colin MADEN[4], and Rainer WIELER[4]

[1]Lund University, Department of Geology, Sölvegatan 12, SE-22362 Lund, Sweden
[2]Department of Physics, Lund University, SE-22100 Lund, Sweden
[3]Department of the Geophysical Sciences, University of Chicago and Chicago Center for Cosmochemistry, Chicago, Illinois 60637, USA
[4]Department of Earth Sciences, ETH Zurich, CH-8092 Zurich, Switzerland
[*]Corresponding author. Email: matthias.meier@geol.lu.se

*(Received 03 May 2013; revision accepted 23 January 2014)*

**Abstract**–We analyzed He and Ne in chromite grains from the regolith breccia Ghubara (L5), to compare it with He and Ne in sediment-dispersed extraterrestrial chromite (SEC) grains from mid-Ordovician sediments. These SEC grains arrived on Earth as micrometeorites in the aftermath of the L chondrite parent body (LCPB) breakup event, 470 Ma ago. A significant fraction of them show prolonged exposure to galactic cosmic rays for up to several 10 Ma. The majority of the cosmogenic noble gases in these grains were probably acquired in the regolith of the LCPB (Meier et al. 2010). Ghubara, an L chondritic regolith breccia with an Ar-Ar shock age of 470 Ma, is a sample of that regolith. We find cosmic-ray exposure ages of up to several 10 Ma in some Ghubara chromite grains, confirming for the first time that individual chromite grains with such high exposure ages indeed existed in the LCPB regolith, and that the >10 Ma cosmic-ray exposure ages found in recent micrometeorites are thus not necessarily indicative of an origin in the Kuiper Belt. Some Ghubara chromite grains show much lower concentrations of cosmogenic He and Ne, indicating that the 4π (last-stage) exposure age of the Ghubara meteoroid lasted only 4–6 Ma. This exposure age is considerably shorter than the 15–20 Ma suggested before from bulk analyses, indicating that bulk samples have seen regolith pre-exposure as well. The shorter last-stage exposure age probably links Ghubara to a small peak of $^{40}$Ar-poor L5 chondrites of the same exposure age. Furthermore, and quite unexpectedly, we find a Ne component similar to presolar Ne-HL in the chromite grains, perhaps indicating that some presolar Ne can be preserved even in meteorites of petrologic type 5.

## INTRODUCTION

The breakup of the approximately 100–200 km sized L chondrite parent body (LCPB) asteroid, about 470 Ma ago, is documented in two different, independent records. First, a large fraction of L chondrites falling today (approximately 70%; Heymann 1967) show radiogenic gas retention ($^{40}$Ar-$^{39}$Ar) ages clustering around 500 Ma (see Keil et al. 1994; and references therein), with the most recent work narrowing in on an age of 470 ± 6 Ma (Korochantseva et al. 2007; Weirich et al. 2012). Second, in a quarry processing mid-Ordovician (467.3 ± 1.6 Ma) limestone near Österplana in southern Sweden, 101 fossil meteorites have been found up to now (Schmitz 2013). These fossil meteorites, the first of which was found in 1987 (Nyström et al. 1988), contain relict meteoritic chromite grains with a major and minor element (Schmitz et al. 1996, 2001) and oxygen isotope (Greenwood et al. 2007; Heck et al. 2010) composition identical to those of chromite grains from recent L chondrites. The two orders of magnitude increase in the number of meteorites reaching Earth at the time, implied by the number of fossil meteorites found in

these sediments, as well as the short cosmic-ray exposure (CRE) ages measured in their relict chromite grains (Heck et al. 2004), is consistent with the interpretation that the fossil meteorites represent debris from the disruption of the LCPB asteroid (Schmitz et al. 2001), which rapidly migrated into Earth-crossing orbits via the 5:2 resonance with Jupiter (Nesvorný et al. 2009).

The orthoceratite limestone at Österplana also contains chromite grains of extraterrestrial origin, dispersed throughout the sediment beds (SEC grains). At several grains per kg of sediment, their concentration is two orders of magnitude higher in the fossil meteorite-bearing layers than in the beds farther down (Schmitz et al. 2003). These SEC grains are again L chondritic in their major and minor element (Schmitz et al. 2003), and oxygen isotopic composition (Heck et al. 2010). Aside from Sweden, similarly high concentrations of SEC grains have recently also been identified in mid-Ordovician rocks from China (Cronholm and Schmitz 2010; Alwmark et al. 2012) and Russia (Korochantsev et al. 2009; Lindskog et al. 2012; Meier et al. 2014), demonstrating that the sudden deposition of many L chondritic SEC grains was a global event. The SEC grains contain He and Ne with an isotopic composition corresponding to that of the (fractionated) solar wind. They have thus been interpreted as "micrometeoritic" dust released in the breakup of the LCPB asteroid and exposed to the solar wind during transfer to Earth (Heck et al. 2008; Meier et al. 2010). In a subset of these SEC grains, "cosmogenic" He and Ne (produced by galactic cosmic rays, GCR) have been found, with individual CRE ages of up to several 10 Ma (Meier et al. 2010), assuming $4\pi$ geometry. Similarly high CRE ages found in recent micrometeorites from polar regions are often thought to reflect long transfer times from original heliocentric distances of 5–150 AU (Olinger et al. 1990; Osawa and Nagao 2002; Trappitsch and Leya 2013), i.e., an initial orbit similar to Jupiter family comets, Jupiter trojan asteroids, Centaurs, or the Kuiper Belt. In contrast, CRE ages of several 10 Ma for micrometeorites from the breakup of the LCPB asteroid cannot represent the transfer time to Earth, as the transfer times of micrometeorites (<200 μm) from the asteroid belt to Earth are limited by Poynting-Robertson drag to the order of <1 Ma (Burns et al. 1979; Heck et al. 2008). Short transfer times (within 1–2 Ma after the LCPB breakup event) are also consistent with rapid deposition of the SEC grains in mid-Ordovician sediment layers. Therefore, Meier et al. (2010) suggested that the approximately 30% of SEC grains with CRE ages in clear excess of typical Poynting-Robertson transfer times were already exposed to GCR in the regolith of the LCPB asteroid, prior to the breakup event. Finding the same high CRE ages in a sample of the LCPB regolith layer would thus not only confirm that regolith-derived grains constitute a significant fraction of the dust produced by the LCPB breakup event but would also suggest that at least some of the long CRE ages observed in recent micrometeorites from polar regions might have been acquired during regolith exposure near the surface of their parent bodies, rather than during transfer from orbits in the Kuiper Belt to Earth.

"Regolith breccia" meteorites are samples of asteroidal regolith: they contain large concentrations of solar wind–derived noble gases and solar flare tracks. Because the solar wind ions penetrate less than 1 μm, and track-inducing heavy solar flare ions penetrate less than 1 cm, track and solar wind–bearing regolith breccia grains must have been residing at some time directly at, or very close to, the surface of their parent asteroid (e.g., Bischoff et al. 2006). Some of these regolith breccia meteorites show a correlation between the concentration of solar wind and cosmogenic Ne in bulk samples (e.g., Fayetteville (H4); Wieler et al. 1989). This "regolith signature" arises probably because grains that spend more time in the topmost 2 m of a well-mixed regolith layer (where they are exposed to GCR) are also more likely to have been exposed directly to the solar wind at the immediate surface. L chondrite regolith breccias are relatively rare: Bischoff and Schultz (2004) report only 12 regolith breccias among 405 L chondrites (3.0%), while in contrast, 15% of all H chondrites are regolith breccias. Among the L chondrite regolith breccias, only Ghubara (L5) is both well studied (Binns 1968; Ferko et al. 2002) and in abundant supply, with more than 200 kg recovered from the Omani desert (Ferko et al. 2002). Ghubara contains two different, main lithologies, namely a light-colored and a dark-colored lithology. The light lithology also contains solar wind noble gases, even more so than the dark lithology (Ferko et al. 2002), thus reversing the roles normally observed in regolith breccias (Suess et al. 1963). Because of solar wind noble gases being present in both light and dark lithologies, Ghubara has been interpreted as a complex "two-generations" regolith breccia (Ferko et al. 2002). Besides the common light lithology with weakly delineated borders (called X1), Ghubara also contains a second light-colored lithology with clearly delineated borders (X2; Binns 1968) and occasional achondritic melt droplets like the ones sampled by Korochantseva et al. (2007). However, given the similar descriptions, it is unclear to us whether the latter two lithologies might actually be the same. While some Ghubara fragments have lost all their trapped He (which is reflected, e.g., in $^4He/^{20}Ne$ ratios of approximately 0.2–2), others have kept larger He


Fig. 1. Picture of the fragment of Ghubara used in this study, with the three samples (Gh1x, Gh2m, Gh3m) indicated. The light lithology from which Gh1x is derived is clearly visible. The unit on the scale bar in the lower left corner is centimeters.

inventories ($^4He/^{20}Ne$ ratios of up to approximately 20), indicating that the relatively large ($R$ = 85 cm) Ghubara meteoroid might have experienced asymmetric gas loss. Both light lithology and dark lithology in Ghubara have about the same bulk CRE ages (15–20 Ma; Ferko et al. 2002). Ghubara further has an Ar-Ar age of 465 ± 6 and 445 ± 24 Ma for melt and light lithology (X1) samples, respectively, and its Ar inventory can be interpreted as an equilibrated mixture of solar and radiogenic Ar mobilized in the LCPB breakup event (Korochantseva et al. 2007). Although this observation suggests that Ghubara is a sample with a rather exceptional history, it also confirms that Ghubara must be a sample of the regolith of the LCPB asteroid that broke up 470 ± 6 Ma ago.

## SAMPLES AND METHODS

### Preparation and Identification of Chromite Grains

We started with a large, fusion-crusted piece (approximately 500 g) of Ghubara, containing both light and dark lithologies (Fig. 1). Numerous pieces of light lithology measure up to 4 cm in diameter. The dark lithology also contains many small, light-colored fragments, making the selection of "pure" dark lithology samples challenging. We prepared three samples. One sample (Gh1x, 4.82 g) derives from a 4 cm sized piece of light lithology of the X1 type: the chondrules are distinct and closely packed, while the border to the dark lithology is not very sharp (Fig. 1). The two other samples derive from the dark lithology (Gh2m, 8.60 g; Gh3m, 7.71 g). The samples were first crushed with a mortar, then dissolved in 3.8 M hydrofluoric acid at room temperature for 1 week, with occasional stirring. After neutralization, the residue was separated into 32–63 μm and >63 μm size fractions, and the larger size fraction was searched for opaque grains using an optical microscope. Candidate chromite grains were analyzed semiquantitatively (on unpolished grain surfaces) for their concentration of Cr, Fe, Mg, Al, Ti, V, Mn, and Zn, using a scanning electron microscope (SEM; Hitachi S3400-N) with an attached energy-dispersive spectrometer (EDS; Oxford Instruments INCAx-sight, calibrated on a Co standard, acceleration voltage was 15 kV), to confirm that their chemical composition corresponds to bona fide chromite. We identified 18, 23, and 39 bona fide chromite grains from samples Gh1x, Gh2m, and Gh3m, respectively. In addition to chromite grains, two Al-rich chromian spinel grains containing up to 30 wt% Al were identified in Gh1x and three in Gh2m. We selected 8 chromite grains and 2 chromian spinel grains from Gh1x, 10 chromite grains and 3 chromian spinel grains from Gh2m, and 12 chromite grains from Gh3m (35 grains in total) for He, Ne analysis. The mass of the grains was measured on a microbalance. This balance has a typical error of approximately 0.2 μg, resulting in relative errors of ≤20% for grains >1 μg. For grains with a mass below 1 μg, the dimensions of the grain were measured on SEM-images and the mass was calculated by multiplying the volume (assuming the vertical axis to be identical to the shorter horizontal axis) with the density of chromite (4.7 g $cm^{-3}$). For these grains, we adopted an error of 30%, which is an empirical value based on the typical deviation observed between inferred and actual volumes of chromite grains previously analyzed with synchrotron X-ray tomographic microscopy (unpublished data).

### Noble Gas Analysis

The grains were individually loaded into holes in an Al sample holder in a noble gas extraction line and pumped at room temperature to ultrahigh vacuum for 48 h. He and Ne were then measured on a custom-built, ultrahigh-sensitivity mass spectrometer using a "compressor source," where a molecular drag pump concentrates the sample gas almost quantitatively into the ion source, thus increasing the sensitivity of the mass spectrometer by up to two orders of magnitude (Baur 1999). The sample gases were released by heating the grains with an infrared (1064 nm) Nd:YAG laser for 30–60 s. The grains melted or, in most cases, slowly vaporized. The released sample gas was passed through two metal-oxide getters and three cryo-traps cooled by liquid nitrogen and containing activated charcoal, to remove background gases and interfering species (in particular $H_2{}^{18}O^+$ and $^{40}Ar^{++}$ on mass 20, and

Table 1. SCR Ne-ratios in ordinary chondritic chromite.

| Rigidity (MV) | Production rate ($10^{-8}$ cm$^3$ STP g$^{-1}$ Ma) $^{21}$Ne | Production rate ratios $^{20}$Ne/$^{22}$Ne$^T$ | $^{21}$Ne/$^{22}$Ne$^T$ | $^{21}$Ne/$^{22}$Ne |
|---|---|---|---|---|
| 50 | 0.117 | 2.66 | 1.12 | 1.09 |
| 75 | 0.148 | 1.86 | 0.755 | 0.749 |
| 100 | 0.175 | 1.51 | 0.653 | 0.661 |
| 125 | 0.198 | 1.33 | 0.620 | 0.632 |
| 150 | 0.218 | 1.23 | 0.610 | 0.623 |

Production rate calculated with the model by Trappitsch and Leya (2013). Production rate ratios indicated with a T were calculated using TALYS-1.2. The $^{21}$Ne/$^{22}$Ne production rate ratio in the rightmost column was calculated from the data by Trappitsch and Leya (2013). All values are based on a composition of 29.8% O, 1.7% Mg, 3.2% Al, 1.7% Ti, 0.5% V, 39.5% Cr, and 21.3% Fe. Fluxes ($J_0$) are set at 100 protons cm$^{-2}$ s$^{-1}$.

$^{(44)}CO_2^{++}$ on mass 22). The electron acceleration voltage was set to 40 V, which additionally suppresses doubly charged ions. Measurements were done according to an established protocol developed and described in detail by Heck et al. (2007). In short, each species is measured in two sequences: one before, and one after laser extraction, each sequence consisting of four to seven cycles of measuring the signals of HD, $^3$He, $^4$He, $H_2O$, $^{20}$Ne, $^{21}$Ne, $^{22}$Ne, $^{40}$Ar, and $CO_2$ in peak-jumping mode. The noble gas amount released by the sample is then determined by the difference between the two sequences extrapolated forward, and backward, respectively, to the moment of extraction. The gas amounts measured in most samples from this study are significantly higher than the typical detection limits for this mass spectrometer as given in Meier et al. (2012). Therefore, only two blank runs were done for this project. The nominal detection limit calculated from the average of these two blanks (i.e., the average gas amount plus two standard deviations of that average, in units of $10^{-15}$ cm$^3$ STP) is approximately 340, approximately 29, approximately 0.18, and approximately 4.9 for $^4$He, $^{20}$Ne, $^{21}$Ne, and $^{22}$Ne, respectively, while $^3$He was not detected in both blanks. These detection limits are similar (except for $^3$He) to the ones reported in Meier et al. (2012). The sensitivity of the mass spectrometer was calibrated using pure standard noble gas mixtures (Heber et al. 2009). The contribution from interfering species to masses 20 and 22 was never larger, and usually much lower than 25% of the ion counting errors of $^{20}$Ne and $^{22}$Ne, and is thus negligible.

## He and Ne Components Used in the Deconvolution Calculations

In the following section, it will become necessary to separate the different He and Ne components that are present in the grains. Here, we define all but one of the components that we will be using. The last component will be defined later, as the need arises.

The composition of SW-Ne retained in Ghubara (GSW component) is defined by the interception of the regression line (in a Ne three-isotope plot) through the bulk data points measured by Ferko et al. (2002) and the SW fractionation line, which connects the SW composition as collected by the Genesis space probe ($^{20}$Ne/$^{22}$Ne = 13.8, $^{21}$Ne/$^{22}$Ne = 0.0329; Heber et al. 2009) with the fractionated solar wind composition as measured, e.g., in lunar samples and micrometeorites (fSW, formerly called SEP; $^{20}$Ne/$^{22}$Ne = 11.2, $^{21}$Ne/$^{22}$Ne = 0.0295; Ott 2002). Hence, the GSW point lies at $^{20}$Ne/$^{22}$Ne = 12.9, $^{21}$Ne/$^{22}$Ne = 0.0317. The GCR component is calculated using the elemental production rate model by Leya and Masarik (2009) for chromite target chemistry (30.1 wt% O, 1.8 wt% Mg, 3.2 wt% Al, 1.6 wt% Ti, 0.7 wt% Mn, 23.8 wt% Fe, and 38.9 wt% Cr; production of $^{21}$Ne from Cr, which is not given in Leya and Masarik [2009], is assumed to be approximately 1.4 times the production of $^{21}$Ne from Fe; see Heck et al. 2004) in an ordinary chondritic matrix and a preatmospheric radius of 85 cm (Ferko et al. 2002). Under these conditions, the $^{20}$Ne/$^{22}$Ne and $^{21}$Ne/$^{22}$Ne ratios range from 0.99 and 0.73, respectively, at the meteoroid surface, to 0.86 and 0.69, respectively, at the center. The calculated concentration of cosmogenic $^{21}$Ne does not depend strongly on the composition of GCR-Ne, so we selected an intermediate $^{21}$Ne/$^{22}$Ne ratio of 0.71, corresponding to a shielding (depth) of 35 cm and a corresponding $^{20}$Ne/$^{22}$Ne ratio of 0.89. The $^{21}$Ne/$^{22}$Ne ratio of solar cosmic-ray-produced Ne (SCR-Ne) was calculated with the elemental production rate model by Trappitsch and Leya (2013). We had to extend that model to also include production of Ne from Cr, as well as the $^{20}$Ne/$^{22}$Ne production rate ratio for all elements (see next subsection). We adopted an intermediate value of $R_0$ = 100 MV (Nishiizumi et al. 2009) for the spectral rigidity, resulting in $^{20}$Ne/$^{22}$Ne = 1.51 and $^{21}$Ne/$^{22}$Ne = 0.653 (Table 1). Ne-HL ($^{20}$Ne/$^{22}$Ne = 8.50; $^{21}$Ne/$^{22}$Ne = 0.0326) is given by Huss and Lewis (1994), while for

our purposes, Ne-E (Amari et al. 1990) can be assumed to be pure $^{22}$Ne.

Assuming the $^{3}$He/$^{4}$He ratio is fractionated to the same extent as Ne (Benkert et al. 1993), we adopt a $^{3}$He/$^{4}$He ratio of $3.25 \times 10^{-4}$ for the GSW component. The GCR $^{3}$He/$^{4}$He and $^{3}$He/$^{21}$Ne ratios for the adopted shielding conditions (as described above) in chromite are 0.230 and 23.0, respectively, clearly different from the same ratios produced by SCR, which are 0.029 and 0.78, respectively (Trappitsch and Leya 2013). For the He-HL component, we use the value of approximately $1.7 \times 10^{-4}$ given by Huss and Lewis (1994).

### Determination of SCR Production Rates

Solar cosmic-ray (SCR) production rates for most target elements relevant for chromite were taken from Trappitsch and Leya (2013), where they were calculated using experimental cross sections. However, no cross section measurements for the production of Ne isotopes from Cr are available. In earlier work studying the GCR-produced Ne content of ordinary chondritic chromite (e.g., Heck et al. 2004, 2008; Meier et al. 2010, 2014), this has not been considered a problem: a large fraction (60–90%; increasing with shielding) of the GCR-Ne is actually produced by Al and Mg, which are present in ordinary chondritic chromite at the level of a few weight-percent (Bunch et al. 1967). The production of $^{21}$Ne from Cr by GCR was assumed to be approximately 1.4 times the production of $^{21}$Ne from Fe (Heck et al. 2004). For SCR, which has a different energy spectrum than GCR, we want to improve on that somewhat simplistic model. As the isotopes of Cr and Fe have a similar abundance pattern and similar neutron excesses, the excitation function for the production of Ne from Cr should have a very similar shape to the experimentally determined one from Fe. However, the threshold energy is expected to shift to lower energies as the mass difference between Cr and Ne is lower than the one between Fe and Ne. Therefore, we expect the threshold energy for the production of Ne from Cr to be lower by four times the binding energy of a nucleon ($4 \times \sim 8.8$ MeV) than the measured threshold energy for the production of Ne from Fe (approximately 129 MeV). We used the experimentally determined excitation function of the $^{nat}$Fe(p,X)$^{21,22}$Ne reaction ("nat" denoting a natural/terrestrial isotopic composition of the respective element) and shifted it by four times the binding energy of an Fe nuclei to lower energies. The threshold energy for Ne production from Cr is then approximately 94 MeV. We then scaled the shifted excitation function to match a $^{nat}$Cr(p,X)$^{21,22}$Ne cross section calculated using INCL-ABLA 4.5 (Boudard et al. 2002) at 3 GeV. The factors by which the two excitation functions were scaled up are 4.9 and 6.3 for $^{nat}$Cr(p,X)$^{21}$Ne and $^{nat}$Cr(p,X)$^{22}$Ne, respectively. To test whether the resulting excitation function is reasonable, we calculate a GCR production rate for $^{21}$Ne from ordinary chondritic chromite of $6.86 \times 10^{-10}$ cm$^3$ STP g$^{-1}$ Ma$^{-1}$ (neglecting shielding) and compare it with the empirically determined $^{21}$Ne production rate from Heck et al. (2008), $7.04 \pm 0.65 \times 10^{-10}$ cm$^3$ STP g$^{-1}$ Ma$^{-1}$ (measured in meteorites with moderate shielding). These two values are in very good agreement, even after taking into account the differences in shielding, which is lower than approximately 25% (Leya and Masarik 2009; $^{21}$Ne production from Cr again scaled to production from Fe). This demonstrates that our adopted Cr excitation function is reasonable. We subsequently used our Cr excitation function to calculate SCR production rates for $^{21,22}$Ne. These results were presented before by Trappitsch and Leya (2012).

To resolve the cosmogenic SCR-Ne from the GCR-Ne, and the solar wind Ne, both $^{20}$Ne/$^{22}$Ne and $^{21}$Ne/$^{22}$Ne in SCR-Ne must be known, but there are no experimentally determined cross sections for the production of $^{20}$Ne from Cr (and other elements). To determine the $^{20}$Ne/$^{22}$Ne ratio, we thus calculated cross sections for the main production paths using the TALYS-1.2 code (Koning et al. 2008). The TALYS code is well suited for calculating the cross sections of interest in the energy range relevant for SCR (<200 MeV; see, e.g., Broeders et al. [2006] for a comparison of different nuclear codes). We therefore prefer it over the INCL-ABLA code for the specific task described here. While the TALYS code has large uncertainties in calculating absolute values of cross sections, they are calculated well relative to each other. This is sufficient, as we are here only interested in production rate ratios to perform an appropriate component deconvolution of our data. Using the calculated cross sections for the main production path of the Ne isotopes, we derived production rate ratios for SCR spectra with different rigidities. Table 1 shows two values for $^{21}$Ne/$^{22}$Ne, one calculated using the TALYS code and one using measured cross sections. A comparison of the two production rate ratios shows excellent agreement within 3% and thus demonstrates the excellent behavior of the TALYS code for calculating cross section ratios as well as the applicability of the described method for calculating the $^{20}$Ne/$^{22}$Ne production rate ratio of SCR-Ne.

## RESULTS

The chromite grains from Ghubara contain both cosmogenic and trapped He and Ne (Table 2). In the

Table 2. Masses, sizes, He, Ne content, and CRE ages of all chromite grains.

| Chromite Grain | Mass (μg) | Size (μm) | $^3He/^4He$ (%) | $^4He$ | $^{20}Ne/^{22}Ne$ | $^{21}Ne/^{22}Ne$ | $^{22}Ne$ | $^3He_{cos}$ | $^{21}Ne_{cos}$ | T3 (GCR) | T21 (GCR) | T21 (SCR) | $^{22}Ne_{pres}$ | Ne-E (%) |
|---|---|---|---|---|---|---|---|---|---|---|---|---|---|---|
| Gh1x | | | | | | | | | | | | | | |
| a1 | 0.4 ± 0.1* | 90 × 70 | 1.30 ± 0.08 | 2.21 ± 0.08 | 8.76 ± 0.47 | 0.27 ± 0.01 | 11.73 ± 0.58 | 27.83 ± 1.4 | 2.88 ± 3.23 | 21.4 ± 2.4 | 51 ± 5.3 | 114 | 1.4 ± 1.1 | – |
| a4 | 1.2 ± 0.0 | 120 × 90 | 1.84 ± 0.13 | 0.67 ± 0.02 | 7.51 ± 0.82 | 0.27 ± 0.03 | 4.74 ± 0.50 | 11.94 ± 0.75 | 1.20 ± 1.35 | 9.2 ± 1.1 | 21.2 ± 2.2 | 115 | 1.7 ± 1.2 | – |
| a5 | 0.4 ± 0.1* | 90 × 70 | 7.06 ± 1.01 | 0.16 ± 0.02 | 1.96 ± 1.39 | 0.42 ± 0.13 | 1.29 ± 0.39 | 11.37 ± 0.82 | 0.53 ± 0.59 | 8.8 ± 1.1 | 9.3 ± 1.1 | 87 | 0.7 ± 0.4 | 65 ± 68 |
| a2 | 0.7 ± 0.2* | 110 × 80 | 1.26 ± 0.08 | 0.48 ± 0.02 | 7.98 ± 0.68 | 0.28 ± 0.02 | 2.82 ± 0.22 | 5.84 ± 0.34 | 0.73 ± 0.82 | 4.5 ± 0.5 | 12.9 ± 1.4 | 49 | 1.0 ± 0.7 | – |
| a3 | 0.5 ± 0.1* | 100 × 70 | 0.69 ± 0.04 | 1.97 ± 0.03 | 11.09 ± 0.42 | 0.1 ± 0.004 | 8.51 ± 0.30 | 12.80 ± 0.65 | 0.58 ± 0.65 | 9.9 ± 1.1 | 10.2 ± 1.1 | 93 | 1.4 ± 0.7 | – |
| a6 | 0.3 ± 0.1* | 80 × 60 | 7.74 ± 3.85 | 0.07 ± 0.03 | 2.52 ± 2.00 | 0.66 ± 0.36 | 1.19 ± 0.64 | 5.50 ± 0.56 | 0.78 ± 0.88 | 4.2 ± 0.6 | 13.8 ± 1.4 | 21 | 0.2 ± 0.5 | 11 ± 206 |
| b1 | 0.3 ± 0.1* | 80 × 60 | 8.34 ± 2.13 | 0.15 ± 0.04 | 1.31 ± 1.21 | 0.56 ± 0.16 | 1.62 ± 0.47 | 12.89 ± 0.79 | 0.90 ± 1.01 | 9.9 ± 1.2 | 16.0 ± 1.7 | 82 | 0.4 ± 0.3 | 73 ± 95 |
| b4 | 27.9 ± 0.0 | 400 × 380 | 1.37 ± 0.02 | 1.1 ± 0.002 | 9.48 ± 0.05 | 0.26 ± 0.003 | 6.71 ± 0.03 | 14.51 ± 0.17 | 1.57 ± 1.76 | 11.2 ± 1.1 | 27.7 ± 2.8 | 19 | 6.3 ± 1.8 | – |
| b2 (Al) | 0.5 ± 0.2* | 100 × 70 | 1.54 ± 0.08 | 0.77 ± 0.02 | 7.64 ± 0.82 | 0.34 ± 0.03 | 4.09 ± 0.40 | 11.72 ± 0.56 | 1.32 ± 1.48 | 8.3 ± 0.9 | 9.4 ± 0.9 | 20 | 0.7 ± 1.1 | – |
| b3 (Al) | 0.5 ± 0.2* | 80 × 80 | 0.69 ± 0.04 | 0.89 ± 0.02 | 9.05 ± 0.72 | 0.23 ± 0.02 | 4.26 ± 0.30 | 5.94 ± 0.36 | 0.89 ± 1.00 | 4.2 ± 0.5 | 6.4 ± 0.7 | 24 | 0.8 ± 0.7 | – |
| **Gh2m** | | | | | | | | | | | | | | |
| c2 | 2.3 ± 0.6 | 150 × 110 | 7.89 ± 0.99 | 0.10 ± 0.01 | 2.96 ± 1.34 | 0.80 ± 0.24 | 0.60 ± 0.18 | 8.04 ± 0.38 | 0.47 ± 0.53 | 6.2 ± 0.7 | 8.3 ± 1.0 | −7 | 0.2 ± 0.4 | −133 ± 419 |
| c1 | 0.7 ± 0.2* | 110 × 80 | 4.11 ± 0.51 | 0.12 ± 0.01 | 4.52 ± 3.71 | 0.75 ± 0.46 | 0.31 ± 0.19 | 5.11 ± 0.33 | 0.23 ± 0.26 | 3.9 ± 0.5 | 4.0 ± 0.4 | −7 | 0.1 ± 0.3 | −160 ± 651 |
| c3 | 3.0 ± 0.0 | 200 × 150 | 9.84 ± 0.75 | 0.12 ± 0.01 | 1.39 ± 0.56 | 0.66 ± 0.08 | 1.12 ± 0.14 | 12.03 ± 0.35 | 0.73 ± 0.82 | 9.3 ± 1.0 | 13.0 ± 1.3 | 36 | 0.9 ± 0.4 | 61 ± 54 |
| c5 | 3.9 ± 0.4 | 200 × 100 | 12.7 ± 0.88 | 0.09 ± 0.01 | 2.00 ± 0.43 | 0.67 ± 0.08 | 0.98 ± 0.12 | 11.24 ± 0.36 | 0.65 ± 0.74 | 8.7 ± 0.9 | 11.6 ± 1.2 | 22 | 1.0 ± 0.5 | 31 ± 50 |
| c6 | 1.0 ± 0.3* | 120 × 90 | 13.0 ± 3.11 | 0.04 ± 0.01 | 4.52 ± 1.01 | 0.38 ± 0.06 | 0.83 ± 0.14 | 5.04 ± 0.26 | 0.30 ± 0.34 | 3.9 ± 0.4 | 5.4 ± 0.5 | 34 | 1.2 ± 0.3 | 16 ± 28 |
| b5 | 3.5 ± 0.4 | 230 × 160 | 13.42 ± 0.94 | 0.09 ± 0.01 | 1.38 ± 0.37 | 0.56 ± 0.08 | 1.22 ± 0.15 | 12.53 ± 0.37 | 0.68 ± 0.76 | 9.7 ± 1.0 | 12.0 ± 1.3 | 61 | 1.6 ± 0.5 | 71 ± 41 |
| b6 | 2.9 ± 0.4 | 130 × 90 | 16.21 ± 1.82 | 0.08 ± 0.01 | 1.75 ± 0.45 | 0.73 ± 0.09 | 1.00 ± 0.12 | 13.21 ± 0.33 | 0.73 ± 0.82 | 10.2 ± 1.0 | 12.9 ± 1.4 | 14 | 0.5 ± 0.3 | 24 ± 67 |
| c4 | 1.2 ± 0.2 | 160 × 120 | 8.61 ± 1.20 | 0.15 ± 0.02 | 1.23 ± 0.8 | 0.75 ± 0.19 | 1.48 ± 0.37 | 12.81 ± 0.64 | 1.10 ± 1.24 | 9.9 ± 1.1 | 19.5 ± 2.0 | 28 | 0.3 ± 0.4 | 55 ± 172 |
| d1 | 1.0 ± 0.3* | 100 × 100 | 10.42 ± 1.89 | 0.05 ± 0.01 | 1.8 ± 1.43 | 0.72 ± 0.23 | 0.42 ± 0.14 | 5.15 ± 0.27 | 0.30 ± 0.34 | 4.0 ± 0.4 | 5.4 ± 0.6 | 7 | 0.2 ± 0.3 | 26 ± 172 |
| d2 | 1.2 ± 0.4* | 120 × 100 | 4.89 ± 0.47 | 0.10 ± 0.01 | 2.28 ± 0.8 | 0.65 ± 0.15 | 0.70 ± 0.16 | 4.64 ± 0.31 | 0.45 ± 0.51 | 3.6 ± 0.4 | 8.0 ± 0.8 | 16 | 0.6 ± 0.5 | 25 ± 84 |
| d3 (Al) | 0.9 ± 0.3* | 120 × 90 | 7.53 ± 0.57 | 0.12 ± 0.01 | 1.10 ± 0.32 | 0.79 ± 0.08 | 2.15 ± 0.22 | 9.30 ± 0.27 | 1.69 ± 1.89 | 6.5 ± 0.7 | 12.0 ± 1.2 | 13 | 0.6 ± 0.5 | 53 ± 100 |
| d4 (Al) | 5.6 ± 0.8 | 220 × 160 | 5.96 ± 0.16 | 0.30 ± 0.01 | 1.60 ± 0.08 | 0.78 ± 0.02 | 3.90 ± 0.11 | 17.56 ± 0.37 | 3.03 ± 3.41 | 12.4 ± 1.3 | 21.6 ± 2.2 | 14 | 2.7 ± 0.6 | 9 ± 23 |
| d5 (Al) | 0.9 ± 0.3* | 140 × 80 | 2.97 ± 0.13 | 0.32 ± 0.01 | 7.95 ± 0.52 | 0.35 ± 0.02 | 2.97 ± 0.17 | 9.58 ± 0.29 | 0.99 ± 1.11 | 6.7 ± 0.7 | 7.0 ± 0.7 | 7 | 0.4 ± 0.8 | – |
| **Gh3m** | | | | | | | | | | | | | | |
| e2 | 4.1 ± 0.1 | 150 × 150 | 11.76 ± 0.59 | 0.13 ± 0.01 | 2.02 ± 0.48 | 0.84 ± 0.13 | 1.01 ± 0.15 | 15.41 ± 0.37 | 0.84 ± 0.95 | 11.9 ± 1.2 | 14.9 ± 1.6 | −7 | 0.3 ± 0.6 | −146 ± 412 |
| d6 | 2.3 ± 0.5 | 200 × 120 | 14.39 ± 1.39 | 0.10 ± 0.01 | 1.90 ± 0.53 | 0.69 ± 0.11 | 1.22 ± 0.20 | 13.69 ± 0.39 | 0.84 ± 0.94 | 10.6 ± 1.1 | 14.9 ± 1.5 | 24 | 0.6 ± 0.5 | 30 ± 76 |
| e5 | 10.3 ± 0.3 | 300 × 210 | 14.49 ± 0.39 | 0.09 ± 0.002 | 1.49 ± 0.14 | 0.85 ± 0.04 | 0.93 ± 0.04 | 13.02 ± 0.19 | 0.8 ± 0.89 | 10.0 ± 1.0 | 14.1 ± 1.4 | −3 | 0.4 ± 0.4 | −118 ± 148 |
| e4 | 6.8 ± 0.1 | 250 × 150 | 13.05 ± 0.40 | 0.11 ± 0.003 | 1.95 ± 0.20 | 0.75 ± 0.04 | 1.16 ± 0.06 | 14.7 ± 0.19 | 0.86 ± 0.97 | 11.3 ± 1.1 | 15.3 ± 1.6 | 10 | 1.3 ± 0.4 | 1 ± 31 |
| e3 | 4.7 ± 0.1 | 210 × 150 | 12.87 ± 0.61 | 0.11 ± 0.004 | 1.66 ± 0.30 | 0.8 ± 0.06 | 1.06 ± 0.07 | 13.56 ± 0.31 | 0.84 ± 0.95 | 10.5 ± 1.1 | 15.0 ± 1.5 | 4 | 0.5 ± 0.3 | −18 ± 68 |
| f4 | 2.7 ± 0.0 | 200 × 110 | 12.71 ± 1.10 | 0.11 ± 0.01 | 2.60 ± 0.58 | 0.55 ± 0.07 | 1.34 ± 0.16 | 13.41 ± 0.34 | 0.72 ± 0.81 | 10.3 ± 1.1 | 12.8 ± 1.3 | 48 | 1.4 ± 0.4 | 35 ± 32 |
| f5 | 1.1 ± 0.1 | 130 × 100 | 13.23 ± 2.28 | 0.10 ± 0.02 | 2.58 ± 0.96 | 0.55 ± 0.12 | 1.54 ± 0.34 | 13.79 ± 0.76 | 0.84 ± 0.94 | 10.6 ± 1.2 | 14.8 ± 1.5 | 56 | 0.7 ± 0.4 | 35 ± 60 |
| f2 | 1.8 ± 0.4 | 180 × 110 | 8.74 ± 0.72 | 0.15 ± 0.01 | 2.27 ± 0.68 | 0.62 ± 0.12 | 1.26 ± 0.25 | 12.8 ± 0.44 | 0.77 ± 0.86 | 9.9 ± 1.0 | 13.6 ± 1.4 | 36 | 0.7 ± 0.4 | 33 ± 66 |
| f1 | 5.1 ± 0.1 | 200 × 150 | 15.46 ± 0.60 | 0.13 ± 0.004 | 1.32 ± 0.25 | 0.83 ± 0.05 | 1.12 ± 0.07 | 19.54 ± 0.49 | 0.92 ± 1.04 | 15.1 ± 1.6 | 16.3 ± 1.7 | 4 | 0.4 ± 0.4 | −4 ± 84 |
| e6 | 2.1 ± 0.0 | 170 × 130 | 14.23 ± 1.24 | 0.12 ± 0.01 | 1.80 ± 0.52 | 0.7 ± 0.12 | 1.59 ± 0.27 | 17.67 ± 0.42 | 1.11 ± 1.25 | 13.6 ± 1.4 | 19.7 ± 2.0 | 31 | 0.7 ± 0.6 | 32 ± 82 |
| e1 | 9.6 ± 0.0 | 200 × 150 | 13.27 ± 0.38 | 0.10 ± 0.002 | 3.12 ± 0.16 | 0.61 ± 0.02 | 1.31 ± 0.04 | 12.71 ± 0.19 | 0.78 ± 0.87 | 9.8 ± 1.0 | 13.8 ± 1.4 | 26 | 4.2 ± 0.4 | 6 ± 10 |
| f6 | 1.0 ± 0.3* | 120 × 90 | 15.47 ± 2.79 | 0.05 ± 0.01 | 1.15 ± 1.02 | 0.82 ± 0.22 | 0.53 ± 0.14 | 7.82 ± 0.35 | 0.43 ± 0.48 | 6.0 ± 0.7 | 7.6 ± 0.8 | 4 | 0.1 ± 0.3 | 30 ± 335 |

Grains labeled with (Al) are Al-rich chromian spinels. Grain masses carrying an asterisk (*) have been calculated from the grain dimensions instead of weighed on a microbalance. An error of "±0.0" in the mass indicates an error smaller than 0.05 μg. All concentrations are given in units of $10^{-8}$ $cm^3$ STP $g^{-1}$, except $^4He$, which is given in $10^{-5}$ $cm^3$ STP $g^{-1}$. The presolar $^{22}Ne$ ($^{22}Ne_{pres}$) amounts are given in $10^{-14}$ $cm^3$ STP. Exposure ages are given in Ma. All errors are 1 sigma.

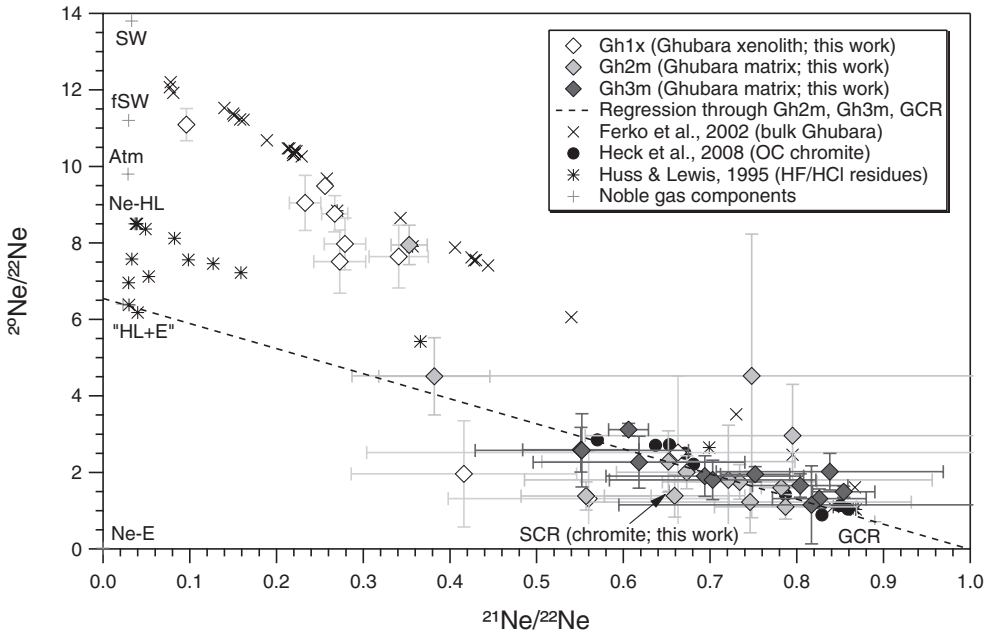


Fig. 2. Ne three-isotope plot. In this and following figures, Ghubara xenolith (Gh1x) chromite grains are represented by white diamonds, Ghubara matrix (Gh2m and Gh3m) chromite grains with light and dark gray diamonds, respectively. The dashed line represents the regression line through the gas-poor dark lithology grains from samples Gh2m and Gh3m, forced through the GCR point. Data for bulk Ghubara analyses from Ferko et al. (2002) are represented by black crosses, chromite batches from recent nonregolithic meteorites from the study of Heck et al. (2008) by black circles. The data from HF/HCl residues by Huss and Lewis (1995) are given as black stars, and finally noble gas components are represented by black pluses. All errors are 1 sigma.

Ne three-isotope diagram (Fig. 2), they form two populations: "gas-rich" (SW-rich), and "gas-poor" (SW-poor) grains. The gas-rich chromite grains derive mostly from the light lithology sample Gh1x, only one grain (Gh2m-d5 (Al)) derives from the dark lithology (it is conceivable that this grain derives from a small fragment of dark lithology in the light lithology sample). The gas-poor chromite grains derive mostly from the dark lithology samples Gh2m and Gh3m, with only three gas-poor grains being from the light lithology. This confirms an observation by Ferko et al. (2002): in a reversal of the roles normally observed in regolith breccias, in Ghubara the light lithology is gas-rich, while the dark lithology is gas-poor. This has been explained with Ghubara being a "two-generations" regolith breccia, i.e., the light lithology probably consists of fragments of a more mature (earlier?) regolith that have been mixed into a (younger?) regolith of lower maturity (Ferko et al. 2002).

The main objective of this study is to determine the concentrations of cosmogenic He and Ne in the Ghubara chromite grains, to compare them with the concentrations of cosmogenic He and Ne in the fraction of SEC grains for which a regolith origin has been proposed (Meier et al. 2010). To calculate the concentrations of cosmogenic $^{3}$He ($^{3}He_{cos}$) and $^{21}$Ne ($^{21}Ne_{cos}$), we first need to determine the fraction of the total $^{3}$He and $^{21}$Ne that has been produced by galactic cosmic rays (GCR). Ferko et al. (2002) were able to do this with a two-component deconvolution, as all their data points in the Ne three-isotope diagram plot essentially on a single mixing line between the solar wind (GSW) and cosmogenic (GCR) components (Fig. 2). However, for the Ghubara chromite grains, the picture is more complex and we need to consider more than two components. For example, the data point of the dark lithology grain Gh2m-c6 is found at an intermediate position between the gas-poor and gas-rich grains, at $^{20}Ne/^{22}Ne = 4.52 \pm 1.01$ and $^{21}Ne/^{22}Ne = 0.382 \pm 0.064$. This point is far away from the mixing line connecting the Ghubara solar wind (GSW) and GCR components (Fig. 2). Furthermore, the remarkably low $^{20,21}Ne/^{22}Ne$ ratios of most of the gas-poor grains cannot be explained by GSW and GCR-Ne alone. They require the presence of a third component, which is enriched in $^{22}$Ne relative to the other two (Fig. 2). Before we can calculate the concentration of $^{3}He_{cos}$ and $^{21}Ne_{cos}$, we therefore first need to identify this third component, and quantify its contribution. We consider essentially two candidates: As many data points of grains from the dark lithology fall rather close to the point representing solar-cosmic-ray-produced Ne

(SCR-Ne; Hohenberg et al. 1978; Reedy et al. 1983; Reedy 1992; this work), we first have to consider whether many Ghubara chromite grains might contain substantial amounts of SCR-Ne. As the penetration depth of SCR is on the order of <2 g $cm^{-2}$ (Hohenberg et al. 1978), less than the size of our piece of Ghubara, our samples Gh1x, Gh2m, and Gh3m cannot have acquired SCR-Ne during transfer to Earth, as they were obviously shielded by surrounding material (Fig. 1). Instead, SCR exposure would have had to take place in the regolith of the LCPB asteroid. As we will show in the discussion section, a significant contribution of SCR-Ne is, however, excluded by other observations. The second candidate for the third component is trapped Ne, as indicated by a regression line through the data points of the gas-poor grains. Extrapolated to $^{21}Ne/^{22}Ne$ approximately 0.03, this regression line passes through a field defined by the Ne composition of "etched" HF/HCl residues measured by Huss and Lewis (1995) in 18 different primitive chondrites (Fig. 2; "etched" residues had their phase Q nobles gases removed by an oxidizing acid). The extrapolated $^{20}Ne/^{22}Ne$ value is lower than for Ne-HL, the Ne component with the lowest $^{20}Ne/^{22}Ne$-value in this region. As the chromite grains from our study have also been prepared by HF-dissolution, this observation leads us to consider a possible contribution of Ne from the presolar components Ne-HL and Ne-E, which dominate the Ne in the residues analyzed by Huss and Lewis (1995). The deconvolution of the Ne data from the gas-poor grains was therefore done using the three components GCR, Ne-HL, and Ne-E as endmembers. For the gas-rich grains, only one additional component can be considered besides the obvious choices GSW and GCR. We define a mixture of Ne-HL and Ne-E as a pseudocomponent "HL+E" when discussing the gas-rich grains. The $^{20}Ne/^{22}Ne$ ratio of HL+E is given by the extrapolation of the regression line through the Ne data points from all gas-poor grains, forced through the GCR point. This regression line intercepts the Ne-fractionation line (Rayleigh fractionation, starting at SW) at $^{20}Ne/^{22}Ne = 6.4 \pm 1.5$ (all other components used have been defined in the Samples and Methods section).

## Cosmogenic Component

In Table 2, we list the $^{3}He_{cos}$ and $^{21}Ne_{cos}$ concentrations of all chromite grains resulting from the three-component deconvolutions. Nominal GCR exposure ages (assuming 4π irradiation geometry) were calculated using the elemental production rates from the Leya and Masarik (2009) model, except for production from Cr, which was fixed as 1.4 times the production from Fe as in Heck et al. (2004). We assume a meteoroid radius of 85 cm (Ferko et al. 2002) and a burial depth (shielding) of 35 cm, close to the maximum production rate for He and Ne for meteoroids of this size. The production rates resulting from this model (in chromite of L chondritic major and minor element composition) are $1.30 \times 10^{-8}$ $cm^3$ STP $g^{-1}$ $Ma^{-1}$ and $5.64 \times 10^{-10}$ $cm^3$ STP $g^{-1}$ $Ma^{-1}$ for $^{3}He$ and $^{21}Ne$, respectively. These numbers are 35% and 20% lower, respectively, than the production rates empirically estimated by Heck et al. (2008) for chromite grains from recent meteorites, which is easily explained by the fact that Ghubara had a larger preatmospheric size than most of the meteorites used to determine the empirical production rates. For the chromian spinel grains, the higher fraction of Al (30%, replacing Cr) increases the (GCR) $^{3}He$ production rate to $1.42 \times 10^{-8}$ $cm^3$ STP $g^{-1}$ $Ma^{-1}$ and the (GCR) $^{21}Ne$ production rate to $1.41 \times 10^{-9}$ $cm^3$ STP $g^{-1}$ $Ma^{-1}$. In Fig. 3, we plot the GCR exposure ages for all analyzed grains. To calculate putative SCR exposure ages, we used a production rate of $1.75 \times 10^{-9}$ $cm^3$ STP $^{21}Ne$ $g^{-1}$ $Ma^{-1}$ for chromite (at a spectral rigidity of $R_0 = 100$ MV and a proton flux-density of $J_0 = 100$ $cm^{-2}$ $s^{-1}$), based on the model by Trappitsch and Leya (2013). No SCR-$^{3}He$ production rates were calculated. The calculated production rate was then linearly scaled to a $J_0$ of 70 $cm^{-2}$ $s^{-1}$ (at 1 AU; Nishiizumi et al. 2009; Hohenberg et al. 1978), and further corrected for the heliocentric distance of the Gefion family of asteroids at 2.8 AU (thought to have been formed in the LCPB breakup event; Nesvorný et al. 2009) assuming an inverse-square dependence of the proton flux-density. This results in a final SCR production rate for $^{21}Ne$ of $1.56 \times 10^{-10}$ $cm^3$ STP $g^{-1}$ $Ma^{-1}$ for chromite, and $3.40 \times 10^{-10}$ $cm^3$ STP $g^{-1}$ $Ma^{-1}$ for chromian spinel, respectively. The nominal (4π) GCR (T3 and T21) and SCR (T21) exposure ages are given in Table 2.

## Trapped Components

The gas-rich chromite grains are dominated by solar wind Ne (>89%) and He (>81%; SW + $^{4}He_{rad}$). The solar wind–derived $^{22}Ne$ concentrations in individual gas-rich chromite grains ($4–10 \times 10^{-8}$ $cm^3$ STP $g^{-1}$) are within one order of magnitude from the Ferko et al. (2002) bulk samples ($6–90 \times 10^{-8}$ $cm^3$ STP $g^{-1}$). The solar wind–derived $^{4}He$ concentrations of $500–2000 \times 10^{-8}$ $cm^3$ STP $g^{-1}$ in the gas-rich grains are higher than in most Ghubara bulk samples measured by Ferko et al. (2002; $100–400 \times 10^{-8}$ $cm^3$ STP $g^{-1}$), but still lower than in bulk samples from gas-rich Ghubara fragments, e.g., BM 1954 and BM 1956 (approximately $3070–14000 \times 10^{-8}$ $cm^3$ STP $g^{-1}$; Ferko et al. 2002;

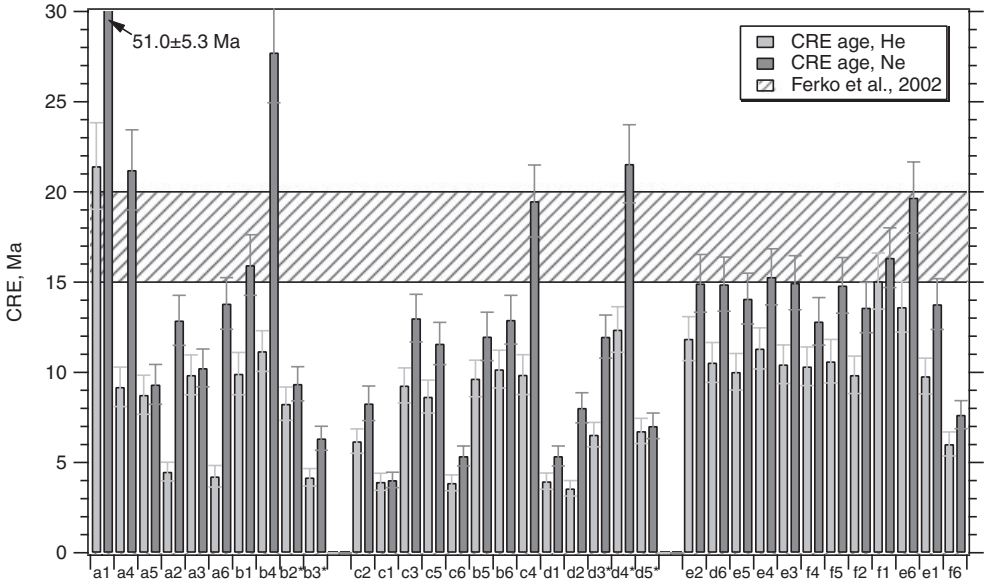


Fig. 3. Cosmic-ray exposure ages calculated from $^{3}$He (light gray) and $^{21}$Ne (dark gray). Grains are grouped by samples, from left to right: 10 samples of Gh1x, 13 samples of Gh2m, 12 samples of Gh3m. All errors are 1 sigma.

Vinogradov and Zadorozhnyi 1965; Levsky 1979; Scherer 1993). Although He is dominated by solar wind (and plausibly some radiogenic $^{4}$He), the cosmogenic contribution is nevertheless clearly visible in the high $^{3}$He/$^{4}$He ratios of the gas-rich grains (0.007–0.018). For the gas-poor grains, on the other hand, the fraction of trapped (and radiogenic) gas fractions to total He and Ne is significantly lower (0–70%, and 20–80%, respectively). This is also visible in the high $^{3}$He/$^{4}$He (0.04–0.16), and $^{21}$Ne/$^{22}$Ne (0.4–0.9) ratios. The trapped $^{22}$Ne concentration in the gas-poor grains (0.06–0.4 $\times$ $10^{-8}$ cm$^{3}$ STP g$^{-1}$) is significantly lower than in the Ghubara bulk samples, while for trapped $^{4}$He (50–150 $\times$ $10^{-8}$ cm$^{3}$ STP g$^{-1}$) the concentration is more similar. The concentrations of the HL+E, and the HL, E components are similar for both gas-rich and gas-poor grains, respectively. In both gas-rich and gas-poor chromite grains, the measured $^{4}$He/$^{20}$Ne ratios are in the range 20–80. While the trapped component shows very low $^{4}$He/$^{20}$Ne ratios (approximately 0–60), indicative of a >90% loss of trapped He, the cosmogenic component shows $^{4}$He/$^{20}$Ne ratios within a factor of approximately 3 of the expected value of 125 (in chromite), indicating an almost quantitative retention of cosmogenic He.

## DISCUSSION

This section is structured as follows: In the first of five subsections, we explore and finally reject the idea of a large contribution of SCR-Ne as an explanation for the low $^{20,21}$Ne/$^{22}$Ne ratios observed in gas-poor Ghubara chromite grains. In the second subsection, we show that the low $^{20,21}$Ne/$^{22}$Ne ratios can instead be explained with a contribution from presolar Ne (Ne-HL, Ne-E). We discuss the CRE history of Ghubara in the third subsection. In the fourth subsection, we compare the He, Ne content of the Ghubara chromite grains with the He, Ne content in SEC grains from mid-Ordovician sediments. In the last subsection, we discuss the presolar Ne component in its own merit.

### A Significant Contribution from SCR Irradiation?

The idea that SCR-Ne may be an important, or even dominating, part of the cosmogenic Ne inventory of many chromite grains in Ghubara is motivated by the observation that in the Ne three-isotope diagram (Fig. 2), the triangle defined by SCR, GSW, and GCR encompasses most of the data points. However, except for shergottites (Garrison et al. 1995) and the Arlington (IIE-an) meteorite (Lavielle et al. 2009), SCR-Ne has not been unambiguously observed in meteorites. SCR-produced radionuclides have been found only in very few meteorites of small preatmospheric size (e.g., Salem [L6]; Nishiizumi et al. 1990) or in rocks from the lunar surface brought back by the Apollo missions (Nishiizumi et al. 2009). In a regolith irradiated by solar and GCR with present-day fluxes, SCR-Ne production dominates GCR-Ne production only in the topmost approximately 2 g cm$^{-2}$ of shielding (at 1 AU; Hohenberg et al. 1978). Hence, if a regolith is well mixed to at least the mean penetration depth of GCR

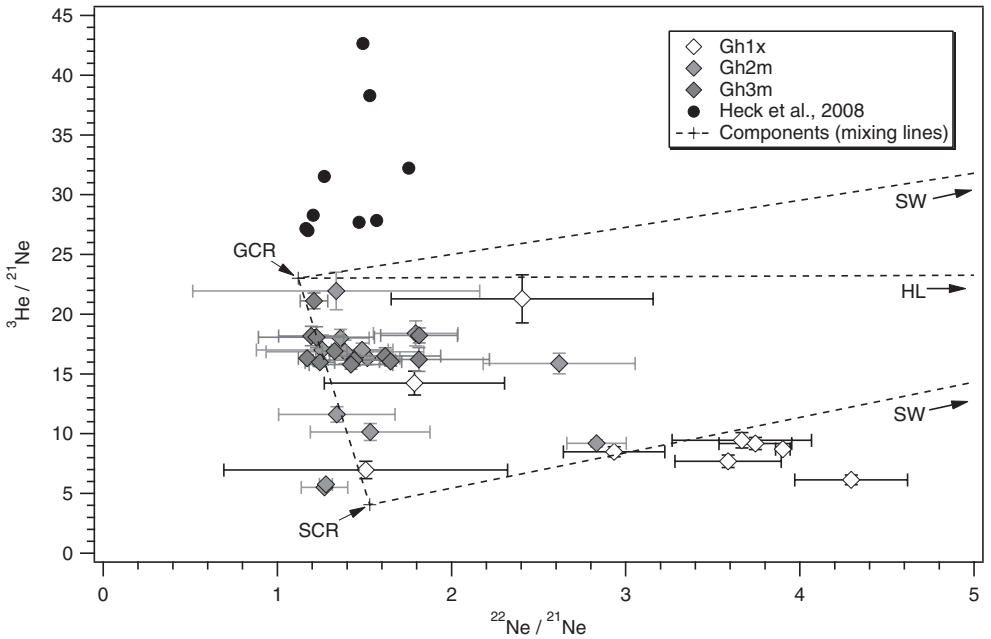


Fig. 4. $^{3}He/^{21}Ne$ versus $^{21}Ne/^{22}Ne$ diagram for Ghubara chromite grains. One grain, Gh1x-a3, plots outside the shown area, at $^{22}Ne/^{21}Ne = 10.4$ and $^{3}He/^{21}Ne = 16.7$. Symbols are identical to the ones used in Fig. 2. Mixing lines between GCR and SW, GCR and SCR, SCR and SW, and GCR and HL are represented by dashed lines. All errors are 1 sigma.

(approximately 100–200 g $cm^{-2}$), the SCR-Ne contribution should be negligible, unless perhaps we were to resort to the hypothesis of an irradiation by an "early active sun" with a strongly increased SCR-flux (e.g., Caffee et al. 1987). In chromite, the hypothesis of a significant contribution from SCR can be tested using the $^{3}He_{cos}/^{21}Ne_{cos}$ and the $^{22}Ne_{cos}/^{21}Ne_{cos}$ ratios, which are clearly different for SCR (3.25 and 1.51, respectively) and GCR (23.0 and 1.12, respectively), as calculated from our SCR production rate model and the model by Leya and Masarik (2009; extended for Cr), respectively. As shown in Fig. 4, there is no correlation between these two ratios in Ghubara chromite grains. Most of the gas-poor (dark lithology) grains plot at the same $^{3}He/^{21}Ne$ value (approximately 17) with no dependence on the $^{22}Ne/^{21}Ne$ ratio. While some of the gas-rich (light lithology) grains plot close to the mixing line between SCR and solar wind in Fig. 4, this must be coincidental: if this mixture is taken at face value, the corresponding SCR exposure ages are much longer than the GCR exposure ages (Table 2), which is impossible. Finally, we note that Heck et al. (2008) measured Ne in chromite grains from five gas-poor (i.e., nonregolithic) ordinary chondrites (Mt. Tazerzait [L5], Harleton [L6], Saint-Séverin [LL6], Eva [H5], and Hessle [H5]). The Ne isotopic ratios measured in these grains plot on almost the same regression line as the gas-poor Ghubara chromite grains (Fig. 2; see next subsection). The low $^{20,21}Ne/^{22}Ne$ ratios are thus not restricted to Ghubara, but are also found in chromite grains from meteorites that were never part of a regolith, and are very unlikely to have retained SCR-Ne due to their large preatmospheric sizes (e.g., 110 kg was recovered from Mt. Tazerzait; Grossmann 1997). For all these reasons, we exclude a significant contribution from SCR-Ne to the Ghubara chromite grains.

### A Nonsolar, Trapped Ne Component in Chromite Grains

We now turn to the alternative explanation for the low $^{20,21}Ne/^{22}Ne$ ratios of the gas-poor grains, involving an additional trapped Ne component in the chromite grains. The regression line through the data points of grains from samples Gh2m and Gh3m, if forced through the GCR point, intersects the Ne-fractionation line (pure Rayleigh fractionation starting at the SW composition) at $^{20}Ne/^{22}Ne = 6.4 \pm 1.5$ and $^{21}Ne/^{22}Ne = 0.022$. This point plots within the field defined by the Ne isotopic composition of etched HF/HCl residues measured by Huss and Lewis (1995) in 18 different primitive chondrites. A similar regression line through the data points of chromite grains from five different ordinary chondrites (Heck et al. 2008), again forced through the GCR point, intersects the same Ne-fractionation line at $^{20}Ne/^{22}Ne = 7.21 \pm 0.57$, within error of the value from the Ghubara samples. The fact that the Ne ratios of chromite grains from both regolithic (Ghubara; this work) and nonregolithic

meteorites (from Heck et al. 2008) plot on the same trend-line demonstrates that this component is unlikely to be explained by the addition of carbonaceous (Ne-HL-rich) matter to the regolith (as suggested, e.g., for howardites; Cartwright et al. 2013). Recently, even some fossil micrometeoritic chromite grains, which plot on the same line, have been reported (Meier et al. 2014). The $^{20}Ne/^{22}Ne$ ratios of $6.4 \pm 1.5$ and $7.21 \pm 0.57$ are somewhat lower than Ne-HL ($^{20}Ne/^{22}Ne$ approximately 8.50; Huss and Lewis 1994), but are compatible with a mix dominated by a trapped component (e.g., Ne-HL, Ne-Q, Ne-P3, Ne-P6, etc.) plus some Ne-E (which can be assumed to be essentially pure $^{22}Ne$ for our purposes; Amari et al. 1990). At present, we cannot show that this component is a mixture at all, nor can we exclude any of the above-mentioned components as part of the mix. As we show in a following subsection, the concentration of Ne-HL+E measured in chromite grains is also far too high to be fractionated Ne-Q origin. If the new component is indeed a mix of presolar Ne-E with any of the above, Ne-HL, Ne-P3, and Ne-P6 would seem to be slightly better choices as they are all presolar, like Ne-E (e.g., Ott 2002). For the moment, we will refer to the new component with the tentative designation "Ne-HL+E" for no other reason than Ne-HL being the presolar component having the most similar Ne isotopic composition to the new component (this does not imply that the component *must* necessarily derive from Ne-HL). We conclude that the simplest explanation for the low $^{20,21}Ne/^{22}Ne$ ratios in the gas-poor chromite grains from Ghubara, and chromite grains from at least five other ordinary chondrites is the addition of small, but measurable, contribution from an unknown, trapped Ne component, possibly a mix of known components plus some Ne-E. The presence of such a component in metamorphic chromite grains from an equilibrated ordinary chondrite is a rather unexpected result. Although presolar nanodiamonds (as well as presolar graphite and SiC grains) are present alongside chromite in HF/HCl residues of primitive (unequilibrated or partially equilibrated) meteorites (e.g., Tang and Anders 1988), presolar Ne-HL and its carrier phases have previously been found to disappear above petrologic grade 3.8 (Huss and Lewis 1995). The detection of a Ne-HL-like Ne component in chromite grains is thus surprising. This will be discussed in a dedicated subsection below. Given that we find the third Ne component present in chromite grains to be trapped, not cosmogenic, the calculation of the GCR-Ne concentration in a conventional three-component deconvolution is justified. We will see in the next subsection that the cosmogenic $^{3}He$ concentrations and exposure ages further support this conclusion.

### The Irradiation History of Ghubara, Told by Chromite

In Fig. 3 (and Table 2), the GCR $^{3}He$ and $^{21}Ne$ exposure ages of all analyzed grains are given. For the values in this figure, we assume GCR irradiation in a meteoroid with a radius of 85 cm and a shielding depth of 35 cm and take the production rates from the model by Leya and Masarik (2009), expanded for Cr. The resulting nominal $4\pi$ CRE ages for each individual grain are similar for He and Ne, although the $^{3}He$-ages tend to be lower (in some cases, up to a factor approximately 3). Lower $^{3}He$ ages (30% lower relative to the $^{21}Ne$ ages) have also been measured in bulk Ghubara samples (Ferko et al. 2002). A He loss of approximately 30% could also explain why many gas-poor chromite grains cluster around a $^{3}He/^{21}Ne$ ratio of approximately 17, instead of the theoretical value of approximately 23.0 (Fig. 4), and would thus bring the $^{3}He$ ages of these grains in accord with $^{21}Ne$ ages. However, some of the grains must have experienced more severe $^{3}He$ losses.

The most remarkable point to be made about Fig. 3 is the large variation in exposure ages between individual grains. The shortest CRE ages are about 4 Ma, while the longest one is >50 Ma, with an average of about 15 Ma. This wide variation can only be explained if the chromite grains were already irradiated in the regolith layer of the LCPB asteroid, prior to the meteoroid stage. This is the same conclusion that was already made for the SEC grains recovered from mid-Ordovician sediments (see next subsection). The CRE age of the Ghubara meteoroid (i.e., the last stage of exposure that delivered Ghubara from its parent asteroid to Earth) must therefore be shorter than the 15–20 Ma implied by the analysis of bulk samples (Ferko et al. 2002). A maximum CRE age for the Ghubara meteoroid is given by the lowest CRE age measured in an individual grain (i.e., assuming this grain has not seen any pre-exposure in the regolith, or had lost all cosmogenic He and Ne before the meteoroid was launched toward Earth). The grain with the lowest CRE age (Gh2m-c1) has identical $^{3}He$ and $^{21}Ne$ ages of $3.93 \pm 0.47$ Ma and $4.04 \pm 0.43$ Ma, respectively (the uncertainties include a 10% error on the production rate). As cosmogenic He would be more readily lost than cosmogenic Ne, we would expect the relative difference between the two CRE ages to increase with increasing loss of cosmogenic gases. Identical $^{3}He$ and $^{21}Ne$ ages therefore imply that He, Ne loss during the last 4 Ma was minimal. This is further corroborated by the observation that no $^{3}He$ age in any Ghubara grain is lower than 4 Ma. Even if we account for the unknown shielding depth (we had assumed 35 cm, but the production rate is up to 40% lower for samples irradiated closer to the surface, or deeper down), the minimum

duration of GCR exposure cannot have been more than 40% longer than this, i.e., some 6 Ma. Therefore, the last-stage (4π) CRE age of Ghubara, i.e., the time it spent in transit from its parent asteroid to Earth, is 4–6 Ma. This is consistent with the observation that all cosmogenic radionuclides measured in Ghubara, including $^{10}$Be, are in saturation (Ferko et al. 2002). The $^{10}$Be/$^{21}$Ne and $^{26}$Al/$^{21}$Ne exposure ages of 15–20 Ma measured by Ferko et al. (2002) in bulk Ghubara samples are therefore only partially due to the last-stage (4π) exposure of the Ghubara meteoroid. The majority of cosmogenic Ne must have been produced during regolith (2π) irradiation. Any differences in exposure age between individual regolith grains disappear in large bulk samples (like the ones measured by Ferko et al. 2002), so that only an average exposure age of the regolith can be calculated for them. The exact duration of the average regolith-irradiation is uncertain, because under 2π irradiation geometry, the GCR production rate (below approximately 50 g cm$^{-2}$), and thus the CRE age, associated with a measured concentration of cosmogenic He or Ne, is a simple function of (an unknown) shielding depth. A minimum duration of regolith exposure can be calculated from the maximum production rate at a shielding of 40–45 g cm$^{-2}$, from the elemental production rate model by Leya et al. (2001) and chromite chemistry (again assuming the elemental production rate from Cr is 1.4 times the production from Fe; Heck et al. 2004). The calculated production rate for chromite ($3.21 \times 10^{-10}$ cm$^3$ STP $^{21}$Ne g$^{-1}$ Ma$^{-1}$) results in an average, minimum regolith-irradiation time of 17 Ma (and up to 81 Ma in one grain).

The CRE age histogram for L chondrites contains a prominent peak at approximately 5 Ma, which is particularly pronounced in meteorites of petrologic type 5 and radiogenic $^{40}$Ar concentrations $<4 \times 10^{-5}$ cm$^3$ STP g$^{-1}$ (Marti and Graf 1992). Ghubara, which is an L5 (Binns 1968) and has a radiogenic $^{40}$Ar concentration of approximately $3 \times 10^{-5}$ cm$^3$ STP g$^{-1}$ (Ferko et al. 2002), fits well into this particular group, in which it represents the first solar gas–rich fragment (Marti and Graf 1992). The asteroid from which this meteorite was launched approximately 5 Ma ago might thus either be a fragment derived from the transition zone between regolith and asteroidal "bedrock," or the parent asteroid might be a rubble pile that reassembled after the breakup event 470 Ma ago from both gas-rich and gas-poor debris.

## Comparison with SEC Grains

The main motivation for this study was the comparison of cosmogenic He and Ne concentrations in chromite grains from an L chondritic regolith breccia with those of sediment-dispersed extraterrestrial chromite (SEC) grains found in mid-Ordovician sediments. Meier et al. (2010) argued that the (4π) CRE ages of typically approximately 15 Ma (and up to 80 Ma) found in SEC grains can only be explained with preirradiation of the grains in the LCPB regolith, as Poynting-Robertson drag requires that SEC grains complete their transfer to Earth in less than 1 Ma. This hypothesis could be tested if we had a sample of the original, prebreakup LCPB regolith, which has not been further irradiated by galactic cosmic-rays (or solar wind) during the last 470 Ma. After correction for the transfer time from the asteroid belt, the chromite grains in such a sample should have the same average cosmic-ray exposure age, and the same exposure age distribution as the preirradiated SEC grains. Do we have a sample of the prebreakup LCPB regolith in our meteorite collections? In the following, we will argue that Ghubara very likely is such a sample, i.e., its solar wind noble gases were entirely acquired prior to 470 Ma ago. Already Korochantseva et al. (2007) noted that Ghubara contains substantial amounts of "remobilized" radiogenic $^{40}$Ar, as well as remobilized solar wind–derived $^{36}$Ar. They suggested that both these Ar components were released from the LCPB during the breakup and then retrapped from a transient atmosphere. In Fig. 5, we present a related argument in favor of a prebreakup age for the Ghubara solar wind noble gases, based on the bulk sample data by Ferko et al. (2002). In most of their samples, $^{40}$Ar and $^{36}$Ar concentrations seem to correlate with each other with a $^{40}$Ar/$^{36}$Ar ratio of about approximately 180 (dashed line in Fig. 5), whereas five remaining samples appear to form their own correlation line with a $^{40}$Ar/$^{36}$Ar ratio of approximately 67 (dash-dotted line in Fig. 5). Both correlation lines pass through the origin within their uncertainties. As $^{40}$Ar and $^{36}$Ar have a different origin, their concentrations should only correlate if they ultimately were acquired by a process that does not differentiate between the isotopes. Retrapping of outgassed (trapped and radiogenic) Ar during the LCPB breakup event is a plausible candidate for such a process. The presence of a retrapped phase is also suggested by the release pattern of Ar at high-temperature steps in the study of Korochantseva et al. (2007). The spread of samples along the correlation lines in Fig. 5 would then arise because different samples of Ghubara retrapped different amounts of Ar. The two different slopes are indicative of two different sources with different $^{40}$Ar/$^{36}$Ar ratios contributing their Ar for retrapping (e.g., layers of regolith with different maturity). The fact that both data arrays extrapolate to the origin in Fig. 5 indicates negligible addition of solar wind Ar (with $^{40}$Ar/$^{36}$Ar < 1) since the retrapping event.

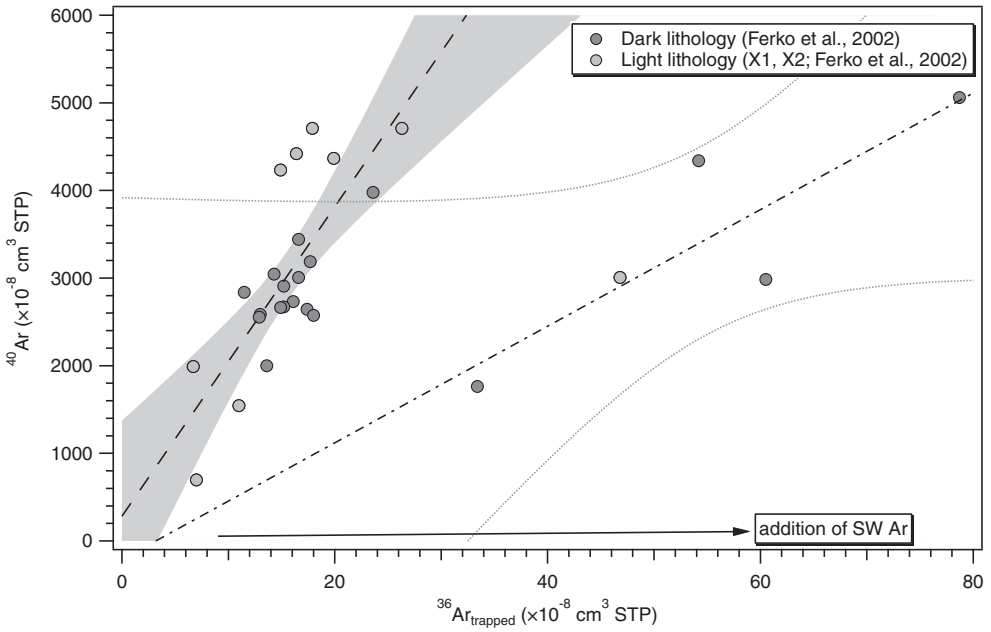


Fig. 5. Argon-40 from radioactive decay of $^{40}$K correlates with $^{36}$Ar from the solar wind. Dark lithology (matrix) and light lithology (xenolith) are represented by light and dark gray symbols, respectively. The dashed line is a linear fit through all the data points along the "correlation" line, while the dash-dotted line is a linear fit through the remaining data points, with the confidence intervals of the fits indicated by the shaded area, and the dotted lines, respectively.

During the last 470 Ma, only about $170 \times 10^{-8}$ cm$^3$ STP $^{40}$Ar/g could have been added by in situ radioactive decay, an amount that cannot be resolved in Fig. 5. We can also consider radiogenic $^4$He. After subtraction of cosmogenic $^4$He (using $^4He_{cos}/^3He_{cos} = 6$; e.g., Leya and Masarik 2009), all samples from Ferko et al. (2002) contain $150 \pm 60 \times 10^{-8}$ cm$^3$ STP $^4$He g$^{-1}$. If this is exclusively radiogenic $^4$He, it corresponds to a U,Th-He age of 520 ± 210 Ma, within error compatible with the LCPB breakup event. Similar to the Ar data, this observation indicates that no solar wind $^4$He was added to Ghubara in the last 470 Ma, and that the regolith sampled by Ghubara is therefore likely to be old, i.e., derived from the regolith of the prebreakup LCPB asteroid.

This means that Ghubara is indeed a viable sample to test the hypothesis that the SEC grains rich in cosmogenic noble gases were pre-exposed in the LCPB regolith. As shown in Fig. 3, individual chromite grains from Ghubara have indeed nominal (4π) CRE ages of approximately 5–20 Ma (and up to 50 Ma). As explained above, we can only give a lower limit for the duration of regolith irradiation due to the unknown shielding depth within the regolith. Therefore, we best compare the concentrations of cosmogenic $^{21}$Ne in Ghubara chromite with the respective values in SEC grains. In Fig. 6, we plot $^{21}Ne_{cos}$ versus $^{20}$Ne in a diagram containing the data from the SEC grains (Meier et al. 2010), Ghubara bulk samples (Ferko et al. 2002), and Ghubara chromite grains from this work. The $^{21}Ne_{cos}$ data of Ghubara bulk samples have been scaled down by a factor of 6.4 to account for the lower $^{21}Ne_{cos}$ production rate in chromite versus bulk L chondrite. From the figure, it is evident that Ghubara chromite grains span the same range of $^{21}Ne_{cos}$ as the SEC grains, except for the addition of approximately $0.3 \times 10^{-8}$ cm$^3$ STP $^{21}$Ne g$^{-1}$ to all Ghubara chromite grains during the approximately 5 Ma last-stage transfer to Earth. It is therefore plausible that the SEC grains and the Ghubara chromite grains shared a common history in the regolith of the LCPB asteroid. The Ghubara bulk data do not show the same variation in $^{21}Ne_{cos}$ as the other two populations (their $^{21}Ne_{cos}$ values are constrained to within $0.5–1.0 \times 10^{-8}$ cm$^3$ STP $^{21}$Ne g$^{-1}$), but this is expected as they represent a large number of individually exposed mineral grains, the contributions of which should average out in bulk samples. Only a fraction of the SEC grains show pre-exposure, with the majority plotting at values <3 Ma (cf. Meier et al. 2010). This has been explained by a major fraction of grains that were never part of the regolith, but derive from the interior of the LCPB and have only been exposed to the solar wind (and GCR) during their <1 Ma transfer to Earth (Meier et al. 2010). In all populations, the bulk of pre-exposed grains has $^{21}Ne_{cos}$ concentrations of up to about 1.2 ×

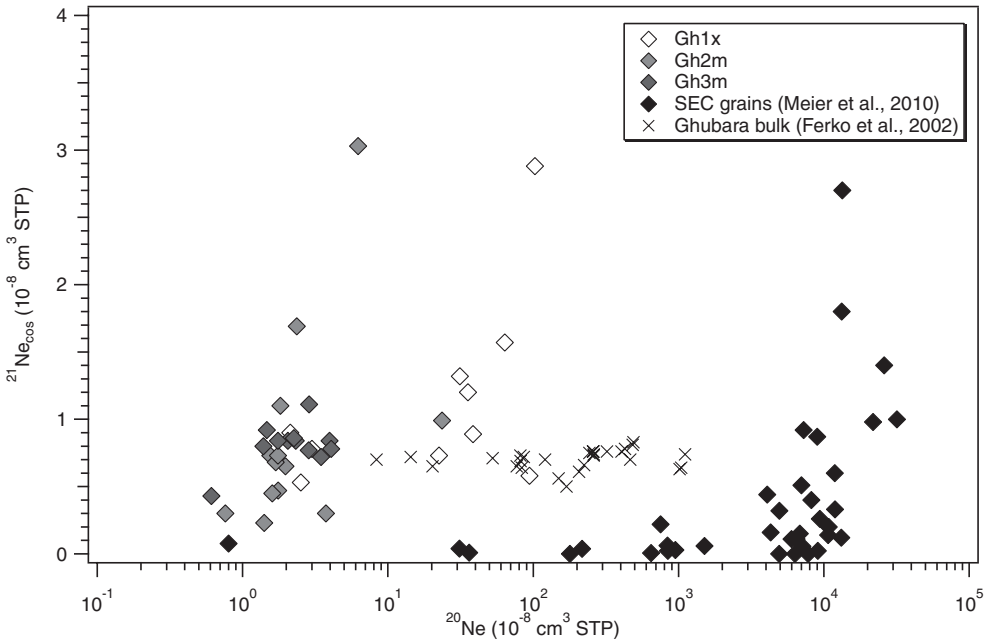


Fig. 6. Cosmogenic $^{21}$Ne versus total $^{20}$Ne, plotted together with data from Meier et al. (2010; black diamonds) and Ferko et al. (2002). All other symbols are identical with the ones used in Fig. 2. The $^{21}Ne_{cos}$ data from Ferko et al. (2002) have been scaled down by a factor of 6.4 to account for the lower $^{21}$Ne production rate in chromite.

$10^{-8}$ cm$^3$ STP g$^{-1}$ (or approximately 37 Ma in the regolith using the $2\pi$ production rate from the last subsection), which is exceeded only by a few grains.

The Ghubara chromite grains are depleted in trapped (SW) $^{20}$Ne by a factor of almost $10^4$ compared with most SEC grains. This observation must be understood in the context of the proposed retrapping event suggested by the Ar data of Ghubara bulk samples, as discussed above. As Ar was almost completely remobilized, the LCPB breakup is likely to have at least partially remobilized Ne as well. However, the cosmogenic Ne in chromite grains was apparently not lost and subsequently retrapped, otherwise the cosmogenic and solar wind inventories of Ne would correlate in the same way as observed for $^{40}$Ar and $^{36}$Ar, which is not the case (Fig. 6). That cosmogenic Ne escaped degassing while solar wind Ne was released is plausible as melting is required to release in situ (cosmogenic, radiogenic) components, and the melting temperature of the major $^{40}Ar_{rad}$ carriers (900–1300 °C; Korochantseva et al. 2007) is too low to melt chromite (melting temperature: >1800 °C), but apparently high enough to release trapped (SW) Ne. The low concentration of $^{20}$Ne in bulk Ghubara samples, compared with the concentration in the SEC grains, must therefore be related to either partial loss or only partial retrapping of solar wind–derived Ne during the LCPB breakup event. Most light lithology chromite grains retained or retrapped a $^{20}$Ne concentration similar to the Ghubara bulk samples from Ferko et al. (2002). On the other hand, most dark lithology grains do not contain any significant fraction of solar wind–derived Ne, suggesting they might never have been exposed to it (e.g., because many of them resided in a large "pebble" within the regolith).

The history of the LCPB regolith that emerges from Fig. 6 starts with a well-mixed regolith layer, with individual grains having $^{21}Ne_{cos}$ concentrations of up to approximately $3 \times 10^{-8}$ cm$^3$ STP g$^{-1}$ and trapped (SW) $^{20}$Ne concentrations on the order of a few times $1000 \times 10^{-8}$ cm$^3$ STP g$^{-1}$. Then, Ghubara loses a large fraction of the trapped $^{20}$Ne in the LCPB breakup event. This event also released the SEC grains from the LCPB (both regolith and nonregolith grains), with their solar wind Ne inventories essentially intact. The SEC grains are transported to Earth as micrometeorites while exposed to a short, additional implantation of SW-Ne, before being deposited in terrestrial sediments. Even today, after 470 Ma in a terrestrial sediment, they are still very rich in SW-derived He and Ne, with concentrations of up to 900 and $30 \times 10^{-5}$ cm$^3$ STP g$^{-1}$ for $^4$He and $^{20}$Ne, respectively (Heck et al. 2008; Meier et al. 2010). These high concentrations of solar wind–derived He and Ne must have been predominantly acquired in the regolith, rather than during transfer to Earth, as the total gas amounts and (pre-)exposure ages of individual SEC grains still correlate with each other (Meier et al. 2010), just as observed, e.g., in the H4 regolith breccia Fayetteville (Wieler et al. 1989). The Ghubara samples, on the other

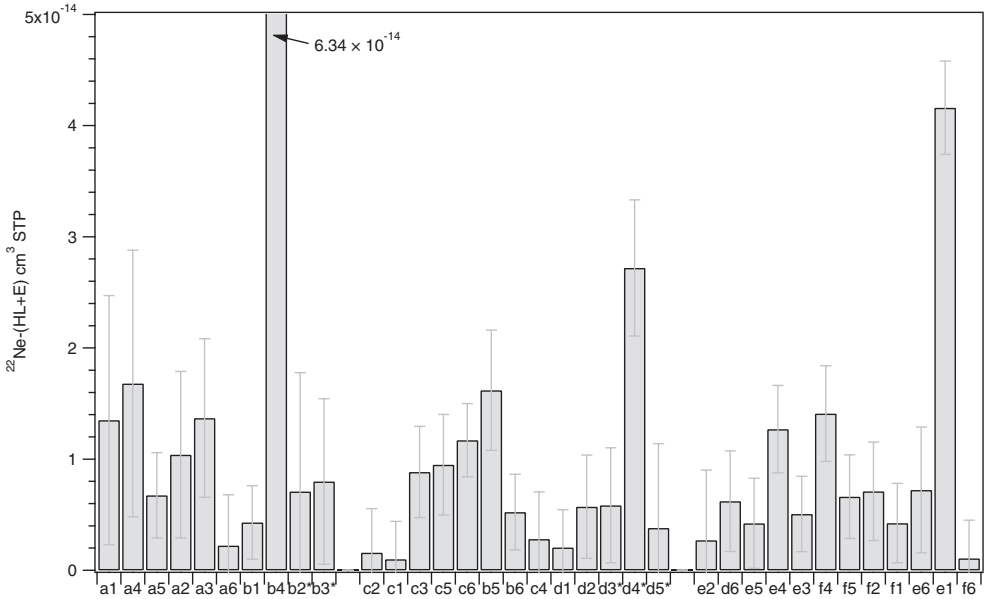


Fig. 7. Presolar $^{22}$Ne amounts calculated by deconvolution for each grain. Grains are grouped by samples, from left to right: 10 samples of Gh1x, 13 samples of Gh2m, 12 samples of Gh3m. All errors are 1 sigma.

hand, spent the next 465 Ma in a fragment from the LCPB breakup, shielded from both solar wind implantation and cosmic-ray exposure, before they were released in a large impact approximately 5 Ma ago, beginning their final transfer to Earth.

## Presolar Ne in Chromite

In Fig. 7, we plot the amounts of $^{22}$Ne-(HL+E) that result from the three-component deconvolution. The average contribution of $^{22}$Ne-(HL+E) is $1.0 \times 10^{-14}$ cm$^3$ STP, with some grains exceeding the average by a factor of up to approximately 6. At an average grain mass of 3.6 μg, this corresponds to a concentration of $2.9 \times 10^{-9}$ cm$^3$ STP $^{22}$Ne-(HL+E) g$^{-1}$ of chromite. Assuming a typical concentration of 0.25% chromite in L5 chondrites (Bunch et al. 1967), this implies a bulk $^{22}$Ne-(HL+E) concentration of $7.1 \times 10^{-12}$ cm$^3$ STP g$^{-1}$, which is far too small to affect bulk analyses. For example, Ghubara contains approximately $10^{-8}$ cm$^3$ STP g$^{-1}$ or a factor >1000 more cosmogenic $^{22}$Ne than $^{22}$Ne-(HL+E). Where does this Ne component come from? The first possibility is fractionated Ne-Q. Ne-Q is the "normal planetary" or "phase Q" component present in many primitive meteorites, and is carried by a so far unidentified carbon-rich carrier (e.g., Busemann et al. 2000; Ott 2002). Ne-Q concentrations in ordinary chondrites decrease with increasing petrologic type (Busemann et al. 2000), and it is conceivable that chromite might retrap part of the remaining, fractionated Ne-Q. Assuming Rayleigh-fractionation only (Ozima et al. 1998), and starting at a value of $^{20}$Ne/$^{22}$Ne = 10.7, the $^{20}$Ne/$^{22}$Ne ratios of 6.4 ± 1.5 and 7.21 ± 0.57 observed in Ghubara and other chromite grains, respectively, correspond to the values expected if the original Ne-Q concentration was depleted by a factor of approximately 37000 and approximately 3300, respectively. As the concentration of Ne-Q in HF/HCl residues of primitive ordinary chondrites is on the order of approximately $10^{-9}$ cm$^3$ STP $^{22}$Ne-Q g$^{-1}$ (Busemann et al. 2000), i.e., similar to the concentration of $^{22}$Ne-(HL+E) in chromite, we can exclude an origin from strongly fractionated Ne-Q. This leaves only two possible explanations: either a mixture of a trapped Ne component (e.g., Ne-Q, Ne-HL, Ne-P3, and/or Ne-P6) with Ne-E, or alternatively a new, so far unknown component. We have not found any literature data on a possible upper limit of $^{22}$Ne-HL (or P3, P6) in ordinary chondrites of type 5, which is not surprising given the conclusion by Huss and Lewis (1995) that presolar Ne is "essentially" gone in meteorites of petrologic type >3.8. Abee (EH4/5) is the only meteorite in the study by Huss and Lewis (1995) having a petrologic type higher than 4, but unfortunately enstatite chondrites are too reduced to contain chromite.

What is the carrier for $^{22}$Ne-(HL+E) in chromite grains in equilibrated meteorites—diamond, or chromite itself? This question is reminiscent of the early years of the decade-long search for the carrier minerals of presolar noble gases. Submicron-sized matrix chromite—the only form of chromite present in unequilibrated

chondrites—was, at the time, one of the leading candidates for the carrier of Ne-HL (e.g., Lewis et al. 1975). Later, it was found that the main carrier of the HL-gases are nanometer-sized, presolar diamonds ("nanodiamonds"; Lewis et al. 1987). The original matrix-normalized concentration of presolar diamond in unequilibrated ordinary chondrites has been calculated to be about 500–1000 ppm, corresponding to a concentration of 0.5–1 $\times$ $10^{-8}$ $cm^3$ STP $^{22}$Ne-HL $g^{-1}$ (Huss and Lewis 1994, 1995). If any nanodiamonds have survived thermal metamorphism in equilibrated chondrites of petrologic type 5, they will also have survived the HF-dissolution step, and might thus be residing on the surface of the individual chromite grains. In a second possibility, some nanodiamonds might have become trapped within the chromite grains as the latter grew during thermal metamorphism (Bunch et al. 1967; Wlotzka 2005), not too dissimilar from the mechanism suspected to produce silicate inclusions in chromite grains (Alwmark and Schmitz 2009; Alwmark et al. 2011). In a third possibility, chromite might have retrapped Ne-HL released from nanodiamonds destroyed during thermal metamorphism. We now use the $^{22}$Ne-HL concentration of 1.0 $\times$ $10^{-5}$ $cm^3$ STP $g^{-1}$ in nanodiamonds given by Huss and Lewis (1994) to calculate the required number of nanodiamonds per chromite grain. An individual, spherical nanodiamond with a radius of 1 nm and a density of 3.5 g $cm^{-3}$ has a mass of 1.5 $\times$ $10^{-20}$ g, and thus contains 1.5 $\times$ $10^{-25}$ $cm^3$ STP $^{22}$Ne-HL (approximately 1 atom of $^{22}$Ne per 2.5 $\times$ $10^5$ nanodiamonds). It therefore takes about 6.8 $\times$ $10^{10}$ of them to account for the 1.0 $\times$ $10^{-14}$ $cm^3$ STP of presolar $^{22}$Ne observed per chromite grain. This adds up to 1.0 ng of nanodiamond per grain, or about 280 ppm for the average 3.6 μg chromite grain. Chromite grains in Ghubara would thus have to be about as abundant in presolar diamond as bulk unequilibrated ordinary chondrites of petrologic type approximately 3.6 (Huss and Lewis 1995). The thus implied bulk abundance of presolar diamond in Ghubara is approximately 0.7 ppm, which is still higher than the matrix-normalized abundances of Julesburg (L3.7), Dimmit (H3.8), and Grady (H3.8) (Huss and Lewis 1995). The surface area of a chromite grain with a mass of 3.6 μg is approximately 4.1 $\times$ $10^{10}$ $nm^2$, while the area covered by a monolayer of 1.0 ng nanodiamond is approximately 27 $\times$ $10^{10}$ $nm^2$, i.e., the nanodiamonds would have to cover several monolayers if they were deposited on the surface of the grains. However, this would require that either the nanodiamonds originally present in the regolith were recovered almost quantitatively on the chromite grains, or that the nanodiamond concentrations in bulk Ghubara are even higher than calculated here. Conversely, in the Ne-HL retrapping scenario, chromite would have to retrap only a part (approximately 30–60%) of the 0.5–1 $\times$ $10^{-8}$ $cm^3$ STP $^{22}$Ne-HL $g^{-1}$ originally present (at 500–1000 ppm concentrations of nanodiamond) to end up with the observed concentration of 2.9 $\times$ $10^{-9}$ $cm^3$ STP $^{22}$Ne-(HL+E) $g^{-1}$. This scenario thus seems more plausible than the two scenarios in which (surface or volume-correlated) diamond is the carrier of Ne-(HL+E). Finally, it is conceivable that many of the metamorphic chromite grains have nebular or even presolar chromite (Zega et al. 2014) at their cores, which might have an exotic (and presently unconstrained) Ne isotopic composition. Currently, we cannot say anything conclusive on the carrier of the Ne-(HL+E) in chromite grains. To improve our understanding of this remarkable finding, future work should extend the study of Ne in chromite grains from ordinary chondrites to meteorites with very low CRE ages (allowing a better resolution of the presolar Ne signal), and also include an analysis of the Xe isotopic composition of these chromite grains, to determine whether it resembles Xe-Q or rather Xe-HL.

## CONCLUSIONS

The main motivation for this study was to compare the $^3$He, $^{21}$Ne cosmic-ray exposure (CRE) ages of chromite grains from Ghubara, a sample of the L chondrite parent body (LCPB) regolith, with those measured in SEC grains retrieved from terrestrial (mid-Ordovician) sediments deposited in the aftermath of the breakup of the LCPB asteroid, to test an earlier hypothesis by Meier et al. (2010) that the >10 Ma CRE ages measured in these SEC grains are due to regolith irradiation on the LCPB asteroid. We confirm this hypothesis by finding a similar range of $^{21}Ne_{cos}$ concentrations in Ghubara chromite grains as in the SEC grains, corresponding to nominal (4π) CRE ages of up to approximately 50 Ma, with an average of 13 Ma, very similar to the corresponding values in the SEC grains (Meier et al. 2010). This also confirms that >10 Ma CRE ages measured in micrometeoroids (e.g., those recovered from polar regions; Olinger et al. 1990; Osawa and Nagao 2002) are not necessarily indicative of a Kuiper Belt origin, as is often suggested. We also find a short 4π (last-stage) irradiation of the Ghubara meteoroid of only 4–6 Ma, much lower than earlier estimates of 15–20 Ma (Ferko et al. 2002), linking Ghubara to a peak in the CRE age histogram of L5 chondrites with low $^{40}$Ar concentrations (Marti and Graf 1992). Ghubara has a remarkable Ar inventory, with clear signs for remobilized (excess) radiogenic $^{40}$Ar and solar wind–derived $^{36}$Ar, as noted before by Korochantseva et al. (2007). Finally, the Ne data of Ghubara chromite grains are suggestive of the presence of a $^{22}$Ne-rich component. We exclude the possibility

that this component is produced by SCR in the Ghubara grains, and propose the existence of a so far unknown Ne component (with $^{20}Ne/^{22}Ne = 6.4 \pm 1.5$) in ordinary chondritic chromite (i.e., not restricted to Ghubara), which we tentatively suggest to be of presolar origin. This surprising observation warrants further investigation.

*Acknowledgments*—We thank E. V. Korochantseva and A. V. Korochantsev for providing a sample of Ghubara for a pilot study (not included here). We also thank P. R. Heck and a second, anonymous reviewer, as well as the associate editor I. Leya, for their comments, which have significantly improved the manuscript. The authors declare no conflicts of interest. This research was supported by the Swiss National Science Foundation (M.M.), the European Research Council (B.S.), the Swedish Research Council (C.A.), and NASA Headquarters (Earth and Planetary Science Fellowship – Grant NNX12AL85H to R.T.), and has made use of NASA's Astrophysics Data System (ADS).

*Editorial Handling*—Dr. Ingo Leya

## REFERENCES

Alwmark C. and Schmitz B. 2009. Relict silicate inclusions in extraterrestrial chromite and their use in the classification of fossil chondritic material. *Geochimica et Cosmochimica Acta* 73:1472–1486.

Alwmark C., Schmitz B., Holm S., Marone F., and Stampanoni M. 2011. A 3-D study of mineral inclusions in chromite from ordinary chondrites using synchrotron microtomography—Method and applications. *Meteoritics & Planetary Science* 46:1071–1081.

Alwmark C., Schmitz B., Meier M. M. M., Baur H., and Wieler R. 2012. A global rain of micrometeorites following break-up of the L-chondrite parent body—Evidence from solar wind-implanted Ne in fossil extraterrestrial chromite grains from China. *Meteoritics & Planetary Science* 47:1297–1304.

Amari S., Anders E., Virag A., and Zinner E. 1990. Interstellar graphite in meteorites. *Nature* 345:238–240.

Baur H. 1999. A noble-gas mass spectrometer compressor source with two orders of magnitude improvement in sensitivity (abstract F1118). *EOS Transactions, AGU* 46: #F1118 (abstr.).

Benkert J.-P., Baur H., Signer P., and Wieler R. 1993. He, Ne, and Ar from the solar wind and solar energetic particles in lunar ilmenites and pyroxenes. *Journal of Geophysical Research* 98:13147.

Binns R. A. 1968. Cognate xenoliths in chondritic meteorites: Examples in Mezö-Madaras and Ghubara. *Geochimica et Cosmochimica Acta* 32:299–306.

Bischoff A. and Schultz L. 2004. Abundance and meaning of regolith breccias among meteorites. *Meteoritics & Planetary Science Supplement* 39:A5118.

Bischoff A., Scott E. R. D., Metzler K., and Goodrich C. A. 2006. Nature and origins of meteoritic breccias. In *Meteorites and the early solar system II*, edited by Lauretta D. S. and McSween H. Y. Jr. Tuscon, Arizona: The University of Arizona Press. pp. 679–712.

Boudard A., Cugnon J., Leray S., and Volant C. 2002. Intranuclear cascade model for a comprehensive description of spallation reaction data. *Physical Review C* 66:044615-1–28.

Broeders C. H. M., Konobeyev A. Y., and Mercatali L. 2006. Global comparison of TALYS and ALICE code calculations and evaluated data from ENDF/B, JENDL, FENDL, and JEFF files with measured neutron induced reaction cross-sections at energies above 0.1 MeV. *Journal of Nuclear and Radiochemical Sciences* 7:N1–N4.

Bunch T. E., Keil K., and Snetsinger K. G. 1967. Chromite composition in relation to chemistry and texture of ordinary chondrites. *Geochimica et Cosmochimica Acta* 31:1569–1582.

Burns J. A., Lamy P. L., and Soter S. 1979. Radiation forces on small particles in the solar system. *Icarus* 40:1–48.

Busemann H., Baur H., and Wieler R. 2000. Primordial noble gases in "Phase Q" in carbonaceous and ordinary chondrites studied by closed system stepped etching. *Meteoritics & Planetary Science* 35:949–973.

Caffee M. W., Hohenberg C. M., Swindle T. D., and Goswami J. N. 1987. Evidence in meteorites for an active early sun. *The Astrophysical Journal Letters* 313:31–35.

Cartwright J. A., Ott U., Mittlefehldt D. W., Herrin J. S., Herrmann S., Mertzman S. A., Mertzman K. R., Peng Z. X., and Quinn J. E. 2013. The quest for regolithic howardites. Part 1: Two trends uncovered using noble gases. *Geochimica et Cosmochimica Acta* 105:395–421.

Cronholm A. and Schmitz B. 2010. Extraterrestrial chromite distribution across the mid-Ordovician Puxi River section, central China: Evidence for a global major spike in flux of L-chondritic matter. *Icarus* 208:36–48.

Ferko T. E., Wang M.-S., Hillegonds D. J., Lipschutz M. E., Hutchison R., Franke L., Scherer P., Schultz L., Benoit P. H., Sears D. W. G., Singhvi A. K., and Bhandari N. 2002. The irradiation history of the Ghubara (L5) regolith breccia. *Meteoritics & Planetary Science* 37:311–327.

Garrison D. H., Rao M. N., and Bogard D. D. 1995. Solar-proton-produced neon in shergottite meteorites and implications for their origin. *Meteoritics* 30:738–747.

Greenwood R. C., Schmitz B., Bridges J. C., Hutchison R., and Franchi I. A. 2007. Disruption of the L chondrite parent body: New oxygen isotope evidence from Ordovician relict chromite grains. *Earth and Planetary Science Letters* 262:204–213.

Grossmann J. N. 1997. The Meteoritical Bulletin 81. *Meteoritics & Planetary Science* 32:A159–A166.

Heber V. S., Wieler R., Baur H., Olinger C., Friedmann T. A., and Burnett D. S. 2009. Noble gas composition of the solar wind as collected by the Genesis mission. *Geochimica et Cosmochimica Acta* 73:7414–7432.

Heck P. R., Schmitz B., Baur H., Halliday A. N., and Wieler R. 2004. Fast delivery of meteorites to Earth after a major asteroid collision. *Nature* 430:323–325.

Heck P. R., Marhas K. K., Hoppe P., and Gallino R. 2007. Presolar He and Ne isotopes in single circumstellar SiC grains. *The Astrophysical Journal* 656:1208–1222.

Heck P. R., Schmitz B., Baur H., and Wieler R. 2008. Noble gases in fossil micrometeorites and meteorites from 470 Myr old sediments from southern Sweden, and new evidence for the L-chondrite parent body break-up event. *Meteoritics & Planetary Science* 43:517–528.

Heck P. R., Ushikubo T., Schmitz B., Kita N. T., Spicuzza M. J., and Valley J. W. 2010. A single asteroidal source for extraterrestrial Ordovician chromite grains from Sweden and China: High-precision oxygen three-isotope SIMS analysis. *Geochimica et Cosmochimica Acta* 74:497–509.

Heymann D. 1967. On the origin of hypersthene chondrites: Ages and shock effects of black chondrites. *Icarus* 6:189–221.

Hohenberg C. M., Podosek F. A., Shirck J. R., Marti K., and Reedy R. C. 1978. Comparisons between observed and predicted cosmogenic noble gases in lunar samples. Proceedings, 9th Lunar and Planetary Science Conference. pp. 2311–2344.

Huss G. R. and Lewis R. S. 1994. Noble gases in presolar diamonds I: Three distinct components and their implications for diamond origins. *Meteoritics* 29:791–810.

Huss G. R. and Lewis R. S. 1995. Presolar diamond, SiC, and graphite in primitive chondrites: Abundances as a function of meteorite class and petrologic type. *Geochimica et Cosmochimica Acta* 59:115–160.

Keil K., Haack H., and Scott E. R. D. 1994. Catastrophic fragmentation of asteroids: Evidence from meteorites. *Planetary and Space Science* 42:1109–1122.

Koning A. J., Hilaire S., and Duijvestijn M. C. 2008. TALYS-1.0. *Proceedings of the International Conference on Nuclear Data for Science and Technology*, Nice, France. pp. 211–214.

Korochantsev A. V., Lorenz C. A., Ivanova M. A., Zaytsev A. V. Kononkova N. N., Roshchina I. A., Korochantseva E. V., Sadilenko D. A., and Skripnik A. Y. 2009. Sediment-dispersed extraterrestrial chromite in Ordovician limestone from Russia (abstract #1101). 40th Lunar and Planetary Science Conference. CD-ROM.

Korochantseva E. V., Trieloff M., Lorenz C. A., Buykin A. I., Ivanova M. A., Schwarz W. H., Hopp J., and Jessberger E. K. 2007. L-chondrite asteroid break-up tied to Ordovician meteorite shower by multiple isochron $^{40}$Ar-$^{39}$Ar dating. *Meteoritics & Planetary Science* 42:113–130.

Lavielle B., Gilabert E., and Marti K. 2009. Solar wind isotopic abundances in 2 mm surface layers of Arlington (abstract #5155). *Meteoritics & Planetary Science* 44: A120.

Levsky L. K. 1979. Redkiye gazi v uglistkikh kondritakh. (Noble gases in carbonaceous chondrites.) *Meteoritika* 38:27–36.

Lewis R. S., Srinivasan B., and Anders E. 1975. Host phase of a strange Xenon component in Allende. *Science* 190:1251–1262.

Lewis R. S., Ming T., Wacker J. F., Anders E., and Steel E. 1987. Interstellar diamonds in meteorites. *Nature* 326:160–162.

Leya I. and Masarik J. 2009. Cosmogenic nuclides in stony meteorites revisited. *Meteoritics & Planetary Science* 44:1061–1086.

Leya I., Neumann S., Wieler R., and Michel R. 2001. The production of cosmogenic nuclides by galactic-cosmic-ray particles for $2\pi$ geometries. *Meteoritics & Planetary Science* 36:1547–1561.

Lindskog A., Schmitz B., Cronholm A., and Dronov A. 2012. A Russian record of a Middle Ordovician meteorite shower: Extraterrestrial chromite at Lynna River, St. Petersburg region. *Meteoritics & Planetary Science* 47:1274–1290.

Marti K. and Graf T. 1992. Cosmic-ray exposure history of ordinary chondrites. *Annual Review of Earth and Planetary Science* 20:221–243.

Meier M. M. M., Schmitz B., Baur H., and Wieler R. 2010. Noble gases in individual L chondritic micrometeorites preserved in an Ordovician limestone. *Earth and Planetary Science Letters* 290:54–63.

Meier M. M. M., Heck P. R., Amari S., Baur H., and Wieler R. 2012. Graphite grains in supernova ejecta—Insights from a noble gas study of 91 individual KFC1 presolar graphite grains from the Murchison meteorite. *Geochimica et Cosmochimica Acta* 76:147–160.

Meier M. M. M., Schmitz B., Lindskog A., Maden C., and Wieler R. 2014. Cosmic-ray exposure ages of fossil micrometeorites from mid-Ordovician sediments at Lynna River, Russia. *Geochimica et Cosmochimica Acta* 125:338–350.

Nesvorný D., Vokrouhlický D., Morbidelli A., and Bottke W. F. 2009. Asteroidal source of L chondrite meteorites. *Icarus* 200:698–701.

Nishiizumi K., Nagai H., Imamura M., Honda M., Kobayashi K., Kubik P. W., Sharma P., Wieler R., Signer P., Goswami J. N., Reedy R. C., and Arnold J. R. 1990. Solar cosmic ray produced nuclides in Salem meteorite. *Meteoritics* 25:392.

Nishiizumi K., Arnold J. R., Kohl C. P., Caffee M. W., Masarik J., and Reedy R. C. 2009. Solar cosmic ray records in lunar rock 64455. *Geochimica et Cosmochimica Acta* 73:2163–2176.

Nyström J. O., Lindstrom M., and Wickman F. E. 1988. Discovery of a second Ordovician meteorite using chromite as a tracer. *Nature* 336:572–574.

Olinger C. T., Walker R. M., Hohenberg C. M., and Maurette M. 1990. Neon measurements of individual Greenland sediment particles—Proof of an extraterrestrial origin and comparison with EDX and morphological analyses. *Earth and Planetary Science Letters* 100:77–93.

Osawa T. and Nagao K. 2002. Noble gas compositions of Antarctic micrometeorites collected at the Dome Fuji Station in 1996 and 1997. *Meteoritics & Planetary Science* 37:911–936.

Ott U. 2002. Noble gases in meteorites—Trapped components. In *Noble gases in geochemistry and cosmochemistry*, edited by Porcelli D. P., Ballentine C. J., and Wieler R. vol. 47. Washington, D.C.: Mineralogical Society of America. pp. 71–100.

Ozima M., Wieler R., Marty B., and Podosek F. A. 1998. Comparative studies of solar, Q-gases and terrestrial noble gases, and implications on the evolution of the solar nebula. *Geochimica et Cosmochimica Acta* 62:301–314.

Reedy R. C. 1992. Should there be solar-proton-produced neon observable in Salem? *Meteoritics* 27:280.

Reedy R. C., Arnold J. R., and Lal D. 1983. Cosmic-ray record in solar system matter. *Science* 219:127–135.

Scherer P. 1993. Einfluss der terrestrischen Verwitterung auf den Edelgasgehalt und die Petrographie von Meteoriten; vergleichende Analysen von Chondriten aus polaren und subtropischen Trockenregionen. Ph.D. thesis, Johannes Gutenberg-Universität Mainz, Germany.

Schmitz B. 2013. Extraterrestrial spinels and the astronomical perspective on Earth's geological record and evolution of life. *Chemie der Erde* 73:117–145.

Schmitz B., Lindström M., Asaro F., and Tassinari M. 1996. Geochemistry of meteorite-rich marine limestone strata

and fossil meteorites from the lower Ordovician at Kinnekulle, Sweden. *Earth and Planetary Science Letters* 145:31–48.

Schmitz B., Tassinari M., and Peucker-Ehrenbrink B. 2001. A rain of ordinary chondritic meteorites in the early Ordovician. *Earth and Planetary Science Letters* 194:1–15.

Schmitz B., Häggström T., and Tassinari M. 2003. Sediment-dispersed extraterrestrial chromite traces a major asteroid disruption event. *Science* 300:961–964.

Suess H. E., Wänke H., and Wlotzka F. 1963. On the origin of gas-rich meteorites. *Geochimica et Cosmochimica Acta* 28:209–233.

Tang M. and Anders E. 1988. Isotopic anomalies of Ne, Xe, and C in meteorites. II. Interstellar diamond and SiC: carriers of exotic noble gases. *Geochimica et Cosmochimica Acta* 52:1235–1244.

Trappitsch R. and Leya I. 2012. Calculation of cosmogenic neon production from chromium. *Meteoritics & Planetary Science Supplement* 75:5089.

Trappitsch R. and Leya I. 2013. Cosmogenic production rates and recoil loss effects in micrometeorites and interplanetary dust particles. *Meteoritics & Planetary Science* 48:195–210.

Vinogradov A. P. and Zadorozhnyi I. K. 1965. Kozmogenniye, radiogenniye i pervichniye inertiye gazi v kamennikh meteoritakh (Cosmogenic, radiogenic and primordial inert gases in stone meteorites). *Meteoritika* 26:77–90.

Weirich J. R., Swindle T. D., and Isachsen C. E. 2012. $^{40}$Ar-$^{39}$Ar age of Northwest Africa 091: More evidence for a link between L chondrites and fossil meteorites. *Meteoritics & Planetary Science* 47:1324–1335.

Wieler R., Baur H., Pedroni A., Signer P., and Pellas P. 1989. Exposure history of the regolithic chondrite Fayetteville. I—Solar-gas-rich matrix. *Geochimica et Cosmochimica Acta* 53:1441–1448.

Wlotzka F. 2005. Cr spinel and chromite as petrogenetic indicators in ordinary chondrites. Equilibration temperatures of petrologic types 3.7 to 6. *Meteoritics & Planetary Science* 40:1673–1702.

Zega T. J., Nittler L. R., Gyngard F., Alexander C. M. O'D., Stroud R. M., and Zinner E. K. 2014. A transmission electron microscopy study of presolar spinel. *Geochimica et Cosmochimica Acta* 124:152–169.